

# The theory of electric dipole moments: the view from below

Jordy de Vries<sup>a,b</sup>

<sup>a</sup>University of Amsterdam, Institute of Theoretical Physics, Science Park 904, 1098 XH Amsterdam, The Netherlands

<sup>b</sup>Nikhef, Theory department, Science Park 105, 1098 XG, Amsterdam, The Netherlands

© 20xx Elsevier Ltd. All rights reserved.

## Abstract

Permanent electric dipole moments (EDMs) of nucleons, nuclei, atoms, and molecules are among the most sensitive probes of CP violation beyond the Standard Model and are intimately connected to the strong CP problem and the origin of the matter-antimatter asymmetry of the universe. This review presents the theory of EDMs from the bottom up, tracing the chain of connections that links CP-violating interactions at level of elementary particles to observable EDMs across a wide range of systems. Starting from a general CP-odd effective Lagrangian at the quark-gluon level comprising the QCD  $\bar{\theta}$  term, quark EDMs and chromo-EDMs, the Weinberg operator, and CP-odd four-fermion interactions, I show how chiral perturbation theory organizes the nonperturbative QCD dynamics into a small set of hadronic low-energy constants, whose relative sizes are determined by the chiral representation of the underlying source. These hadronic interactions feed into calculations of nuclear EDMs and Schiff moments, which in turn enter atomic and molecular structure calculations that connect to experimentally accessible observables in diamagnetic and paramagnetic systems. Special attention is given to the recently identified sensitivity of paramagnetic systems to hadronic CP violation, which opens a new and relatively unexplored window on the quark-gluon sector. The complementarity of the full EDM portfolio including the neutron, light nuclei, atoms, and molecules, and the role of theory in disentangling the underlying source of CP violation is discussed throughout.

## 1 Introduction

Permanent electric dipole moments (EDMs) of elementary particles, nucleons, nuclei, atoms, and molecules are among the most sensitive probes of CP violation available. An EDM is the analogue of a magnetic dipole moment, but instead of the coupling between spin and a magnetic field it couples to an electric field. Its existence requires both parity (P) and time-reversal (T) violation, and by the CPT theorem, CP violation. Due to its flavor structure, the single known source of CP violation in the quark-mixing matrix, predicts EDMs that are extraordinarily small, many orders of magnitude below current experimental sensitivity. Therefore, any EDM observed in the foreseeable future would be unambiguous evidence for new sources of CP violation. This is not idle hope as additional CP violation is expected to exist to explain the asymmetry between matter and antimatter in our universe.

The experimental landscape has advanced significantly in recent years. The best limit on the electron EDM,  $|d_e| < 4.1 \times 10^{-30}$  e cm, comes from precision spectroscopy of the polar molecule  $\text{HfF}^+$  (Roussy et al. (2023)), with competitive results from  $\text{ThO}$  (Andreev et al. (2018)). The neutron EDM is bounded at  $|d_n| < 1.8 \times 10^{-26}$  e cm (Abel et al. (2020)), and the diamagnetic atom  $^{199}\text{Hg}$ ,  $d_{^{199}\text{Hg}} < 7.4 \cdot 10^{-30}$  e cm, provides the tightest constraint on hadronic CP violation in heavy nuclei (Graner et al. (2016)). Next-generation experiments, including new molecular EDM searches, improved neutron EDM measurements, storage ring experiments targeting proton and nuclear EDMs, and searches in radioactive species such as  $^{225}\text{Ra}$  and  $\text{RaF}$ , aim to improve the sensitivity over the coming decade (Alarcon et al. (2022)). While the experimental limits in these classes differ by several orders of magnitude, their sensitivity to underlying quark, gluon, and semi-leptonic operators is often comparable, owing to a web of enhancement and suppression factors associated with finite-size effects, violations of Schiff shielding, nuclear collectivity, and molecular polarization. Navigating this web, and ultimately interpreting a future EDM signal in terms of a specific source of CP violation, requires a quantitative theoretical framework connecting fundamental CP violation to hadronic, atomic, and molecular observables, see Fig. 1. The aim of this review is to describe that framework.

EDMs are intimately connected to the strong CP problem, one of the fine-tuning puzzles in the Standard Model (SM). The QCD Lagrangian admits a CP-violating term proportional to  $\bar{\theta}$ , the sum of the vacuum angle and the argument of the quark mass determinant. Experimental bounds on the neutron EDM constrain  $|\bar{\theta}| \lesssim 10^{-10}$ , yet there is no symmetry reason within the SM for  $\bar{\theta}$  to be this small. The most elegant solution is the Peccei-Quinn mechanism (Peccei and Quinn (1977)), which promotes  $\bar{\theta}$  to a dynamical field relaxed to zero by a new pseudo-Nambu-Goldstone boson, the axion. EDM experiments are sensitive to  $\bar{\theta}$  directly, and as discussed in this review, the pattern of EDMs across different systems might reveal whether the strong CP problem is solved by an axion mechanism or in some other way.

The network of connections between microscopic CP-odd sources and EDM observables is naturally described within an effective field theory (EFT) framework. At and above the electroweak scale, one writes a general CP-odd EFT in terms of SM fields, organized in operators of increasing dimension, and matches this onto a basis of quark, gluon, and lepton operators at a hadronic scale of order 1–2 GeV. A recent review (Pospelov and Ritz (2025)) provides a broad overview of EDMs as probes of physics beyond the SM (BSM), emphasizing this operator basis at and above the electroweak scale and the connection to a wide range of ultraviolet (UV) models such as supersymmetry, extended Higgs sectors, neutrino portals, and dark sectors. Another recent review has focused on the role of EDMs in testing electroweak baryogenesis (van de Vis et al. (2026)).

The present review is intended as a complement to these particle physics and cosmological perspectives. While a bird's eye view sees the big picture and surveys the broad landscape of BSM scenarios, the worm's eye view from the mud of hadronic, nuclear, atomic, and

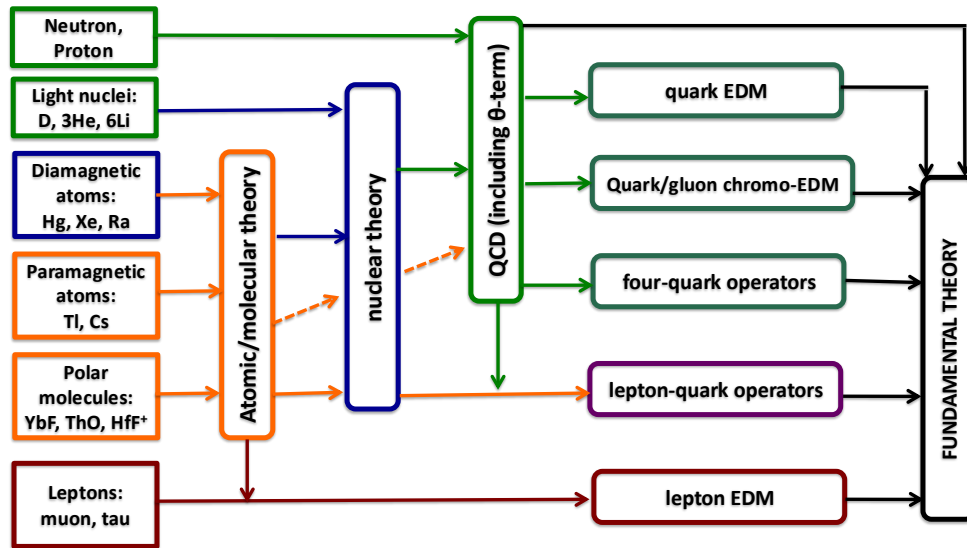


Fig. 1: The EDM ‘metro map’ showing how to connect the EDM measurements (left) to the fundamental theory of CP violation (right) by going through molecular, atomic, nuclear, and hadronic theory. Effective operators such as quark EDMs and chromo-EDMs are used as intermediate steps. The dashed orange arrows show connections that are recently identified and reviewed in Sect. 6.1.

molecular physics can reveal structures that are invisible from the top. Rather than surveying UV model space, I therefore concentrate on the hadronic, nuclear, and atomic/molecular layers of the EFT hierarchy that connect CP-violating sources at level of elementary particles to the EDMs of nucleons, nuclei, atoms, and molecules. The starting point is an effective CP-odd Lagrangian formulated at a renormalization scale around a few GeV, containing the QCD  $\theta$ -term, quark and lepton EDMs, quark chromo-EDMs, the three-gluon (Weinberg) operator, and CP-violating four-fermion operators. Below this scale, the appropriate degrees of freedom are hadrons rather than quarks and gluons, and nonperturbative QCD is encoded in the couplings of a chiral EFT involving pions, nucleons, and heavier baryons. The hadronic interactions in turn feed into nuclear many-body calculations, which determine the EDMs and Schiff moments of nucleons, light and heavy nuclei, and ultimately into atomic and molecular structure calculations that connect to atomic and molecular EDMs. Throughout, I emphasize the progress made based on EFTs and modern nuclear and atomic/molecular many-body methods, which aims to organize these steps in a controlled expansion and to provide a consistent language for comparing different systems and sources. I put extra emphasis on recent work connecting hadronic CP violation to paramagnetic systems as this is still rather unexplored territory.

## 2 CP-violating effective interactions at low energy

The interpretation of EDM searches in terms of fundamental sources of CP violation involves a multitude of scales ranging from molecular (eV) to BSM physics (TeV or beyond). Above the electroweak scale, the appropriate language is the Standard Model Effective Field Theory (SMEFT) (Buchmuller and Wyler (1986), Grzadkowski et al. (2010)), in which BSM physics at a scale  $\Lambda \gg v$  is integrated out and encoded in a tower of  $SU(3)_c \times SU(2)_L \times U(1)_Y$  gauge-invariant operators built from SM fields. CP-odd effects first appear at dimension six, so the leading BSM contributions to CP violation carry a suppression  $v^2/\Lambda^2$  relative to the SM, where  $v \simeq 246$  GeV is the Higgs vacuum expectation value. The requirement of full gauge invariance is a powerful constraint on the operator basis and strongly constrains the possible CP-odd interactions.

The effective SMEFT operators involve the full SM field content. Below the electroweak scale, heavy degrees of freedom such as the Higgs, top quarks, and electroweak gauge bosons, are integrated out, leaving a tower of local CP-odd operators built from light SM fields. Renormalization-group (RG) evolution from the electroweak scale down to  $\mu \sim 1$ -2 GeV, where quarks and gluons are matched onto hadronic degrees of freedom, reshuffles these operators and generates a correlated ensemble of Wilson coefficients, see Sect. 2.6 for a discussion. At the hadronic matching scale, around 2 GeV, the CP-violating Lagrangian takes the form

$$\mathcal{L}_{\text{CPV}} = \mathcal{L}_{\bar{\theta}} + \mathcal{L}_{d_q} + \mathcal{L}_{\bar{d}_q} + \mathcal{L}_W + \mathcal{L}_{A_q} + \mathcal{L}_{d_e} + \mathcal{L}_{s_1} + \dots, \quad (1)$$

where the dots denote higher-dimensional operators. In this section I introduce each term in turn, with enough detail to map to a theory of hadronic CP violation in Sect. 3.

## 2.1 The QCD $\bar{\theta}$ term

The only CP-odd interaction of dimension four in QCD is the topological term ('t Hooft (1976))

$$\mathcal{L}_{\bar{\theta}} = -\bar{\theta} \frac{g_s^2}{32\pi^2} G_{\mu\nu}^a \tilde{G}^{a\mu\nu}, \quad (2)$$

where  $G_{\mu\nu}^a$  is the gluon field-strength tensor,  $\tilde{G}^{a\mu\nu} = \frac{1}{2}\epsilon^{\mu\nu\alpha\beta}G_{\alpha\beta}^a$  its dual, and  $\bar{\theta} = \theta_{\text{QCD}} + \arg \det M_q$  is the physical combination of the QCD vacuum angle and the phase of the quark-mass matrix  $M_q$ . The operator  $G\tilde{G}$  is a total derivative and has no perturbative effects, but leads to non-perturbative hadronic matrix elements contributing to, for example, the neutron EDM.

The strong CP problem is the question of why  $|\bar{\theta}| \lesssim 10^{-10}$ , as required by the neutron EDM bound (Abel et al. (2020)). While several mechanisms have been proposed to explain why  $\bar{\theta}$  is so small,  $\bar{\theta}$  remains a legitimate free parameter of the low-energy theory. Even when a Peccei-Quinn (Peccei and Quinn (1977)) mechanism is present, an effective  $\bar{\theta}$  is induced by other CP-odd sources present in the theory once the axion field takes its minimum value (see for example Pospelov and Ritz (2001) and Dekens et al. (2022)). The hadronic consequences of the  $\bar{\theta}$  term must be understood in any case.

The gluonic term in  $\mathcal{L}_{\bar{\theta}}$  can be traded, via an axial  $U(1)$  rotation of the quark fields, for a complex contribution to the quark mass matrix

$$\mathcal{L}_{\bar{\theta}} \longrightarrow \bar{\theta} m_* \bar{q} i \gamma_5 q, \quad (3)$$

where  $q = (u d)^T$  and  $m_* = m_u m_d / (m_u + m_d)$  is the reduced quark mass. This form makes the chiral transformation properties explicit: the  $\bar{\theta}$  term acts as an imaginary quark mass, vanishes in the chiral limit, and conserves isospin.

## 2.2 Quark EDMs and chromo-EDMs

The quark electric dipole moments (qEDMs) are dimension-five dipole operators

$$\mathcal{L}_{d_q} = -\frac{i}{2} \sum_{q=u,d,s} d_q \bar{q} \sigma^{\mu\nu} \gamma_5 q F_{\mu\nu}, \quad (4)$$

where  $F_{\mu\nu}$  is the electromagnetic field strength. The qEDM is a chirality-odd operator that transforms in the same chiral representation as the quark mass matrix, but it is tied to the electromagnetic current. As a consequence, at hadronic scales it primarily induces operators with explicit photons, such as nucleon EDMs, while purely hadronic interactions are suppressed by  $\alpha_{\text{em}}$ . This makes the qEDM phenomenologically distinct from the  $\bar{\theta}$  term and quark chromo-EDMs (qCEDMs) despite sharing the same chiral representation.

The quark chromo-EDMs are the gluonic analogs of the qEDMs

$$\mathcal{L}_{\bar{d}_q} = -\frac{i}{2} \sum_{q=u,d,s} \bar{d}_q \bar{q} \sigma^{\mu\nu} \gamma_5 t^a q g_s G_{\mu\nu}^a, \quad (5)$$

with  $t^a$  the  $SU(3)_c$  generators. The qCEDMs share the chiral transformation properties of the  $\bar{\theta}$  term and quark masses, but couple to gluons rather than photons. Their low-energy phenomenology is therefore much closer to that of the  $\bar{\theta}$  term. An important difference is that the qCEDMs can break isospin if  $\bar{d}_u \neq \bar{d}_d$ .

It is important to stress that, although Eqs. (4) and (5) are dimension-five operators in the low-energy QCD+QED theory, they originate from *dimension-six* operators in the Standard Model EFT (SMEFT). The reason is that above the electroweak scale the theory is invariant under  $SU(2)_L \times U(1)_Y$ , so chirality-flipping dipole operators must involve the Higgs field. The Wilson coefficients  $d_q$  and  $\bar{d}_q$  are therefore effectively suppressed as  $v/\Lambda^2$  where  $\Lambda$  is the BSM scale. In many explicit BSM scenarios an additional small Yukawa coupling appears effectively replacing  $v \rightarrow m_q$ , the light quark mass, but this is not true for all scenarios (Dekens et al. (2019)). The CP-odd quark dipoles are induced in many BSM models. Perhaps the most famous example is supersymmetry where they can be induced at one loop already through the exchange of virtual supersymmetric particles (Ellis et al. (1982); Buchmuller and Wyler (1983)).

## 2.3 The Weinberg three-gluon operator

The CP-odd three-gluon (Weinberg) operator is the unique dimension-six purely gluonic CP-violating operator (Weinberg (1989))

$$\mathcal{L}_W = \frac{C_W}{6} f^{abc} \epsilon^{\alpha\beta\mu\nu} G_{\alpha\beta}^a G_{\mu\rho}^b G_{\nu\rho}^c, \quad (6)$$

with  $f^{abc}$  the  $SU(3)_c$  structure constants. The Weinberg operator can be interpreted as the chromo-electric dipole moment of the gluon (Braaten et al. (1990)). Unlike the  $\bar{\theta}$  term,  $\mathcal{L}_W$  generates CP-odd vertices at the perturbative level and does not vanish in the chiral limit. Because it involves only gluon fields and no quark bilinears, the Weinberg operator conserves chiral symmetry making its low-energy phenomenology rather different from the  $\bar{\theta}$  term and q(C)EDMs. The Weinberg operator is induced after integrating out heavy quarks with a qCEDM (Braaten et al. (1990)) and thus appear often together with q(C)EDMs. It can also be generated in multi-Higgs (Weinberg (1989)) and leptoquark models (Abe et al. (2018)).

## 4 The theory of electric dipole moments: the view from below

### 2.4 Four-quark operators

At dimension six, flavor-diagonal four-quark operators provide two physically distinct classes of CP-odd sources. The first class consists of chiral-invariant operators of the form

$$\mathcal{L}_{4q}^{(q\text{-inv})} \sim C_{4q}^{(1)} [(\bar{q}q)(\bar{q}i\gamma_5 q) - (\bar{q}\vec{\tau}q) \cdot (\bar{q}\vec{\tau}i\gamma_5 q)] + C_{4q}^{(8)} [(\bar{q}t^a q)(\bar{q}i\gamma_5 t^a q) - (\bar{q}\vec{\tau} t^a q) \cdot (\bar{q}\vec{\tau}i\gamma_5 t^a q)], \quad (7)$$

where  $q = \{ud\}^T$ . More operators appear once strange quarks are included. The operators in Eq. (7) share a common low-energy phenomenology with the Weinberg operator. They are generated directly in the SMEFT from four-quark operators and are for example induced in leptoquark models (Dekens et al. (2019)).

The second and phenomenologically more distinctive class is the four-quark left-right (FQLR) operator (Ng and Tulin (2012))

$$\mathcal{L}_{4q}^{(\text{LR})} = C_{\text{LR}} i (\bar{u}_R \gamma^\mu d_R \bar{d}_L \gamma_\mu u_L - \bar{d}_R \gamma^\mu u_R \bar{u}_L \gamma_\mu d_L) + \dots \quad (8)$$

where the dots denote similar operators with different color structure and/or strange quarks. The FQLR transforms as  $(3_L, 3_R)$  under  $SU(2)_L \times SU(2)_R$ , which is a fundamentally different chiral representation than the  $\bar{\theta}$  term or the qCEDMs, leading to a qualitatively different low-energy phenomenology. The FQLR is not a direct SMEFT operator but is induced after electroweak symmetry breaking from the SMEFT operator  $i(\bar{H}^\dagger D_\mu H)(\bar{u}_R \gamma^\mu d_R) + \text{h.c.}$ , which generates a coupling of the  $W$ -boson to right-handed quarks. Integrating out the  $W$ -boson then produces Eq. (8). This operator dominates EDM phenomenology in left-right symmetric models (Xu et al. (2010)).

### 2.5 Lepton EDMs and semi-leptonic operators

The electron EDM (and analogously the muon and tau EDM)

$$\mathcal{L}_{d_e} = -\frac{i}{2} d_e \bar{e} \sigma^{\mu\nu} \gamma_5 e F_{\mu\nu}, \quad (9)$$

is the primary target of paramagnetic EDM experiments and is a purely leptonic CP-odd source. It is generated in the SMEFT from the similar dimension-six operators as the qEDM, after inserting a Higgs vev. It appears in similar BSM scenarios as the qEDMs and qCEDMs.

Beyond the electron EDM, atomic and molecular EDMs are also sensitive to CP-odd interactions between electrons and quarks. At dimension six, three classes of dimension-six semi-leptonic operators are relevant for EDM phenomenology, distinguished by their Lorentz structure

$$\mathcal{L}_{\text{sl}} = \bar{e} i \gamma^5 e (c_S^{(0)} \bar{q} q + c_S^{(1)} \bar{q} \tau^3 q) + \bar{e} i \sigma^{\mu\nu} \gamma^5 e (c_T^{(0)} \bar{q} \sigma_{\mu\nu} q + c_T^{(1)} \bar{q} \sigma_{\mu\nu} \tau^3 q) + \bar{e} e (c_P^{(0)} \bar{q} i \gamma^5 q + c_P^{(1)} \bar{q} i \gamma^5 \tau^3 q). \quad (10)$$

Similar to the chiral-invariant four-quark operators these operators appear directly in SMEFT from four-fermion operators and arise, for example, from tree-level leptoquark exchange (Dekens et al. (2019); Fuyuto et al. (2019)). Similar couplings to heavier quarks can be written which, after integrating out the heavy quarks, leads to operators of the form  $\bar{e} e G_{\mu\nu}^a \tilde{G}^{\mu\nu,a}$  and  $e \vec{\tau} \gamma^5 e G_{\mu\nu}^a G^{\mu\nu,a}$ . The hadronization of the semi-leptonic operators, discussed in more detail below, is relatively straightforward and mainly leads to operators of the same form as in Eq. (10) but replacing  $q \rightarrow N$ , where  $N = \{pn\}^T$  is the nucleon doublet.

### 2.6 Renormalization-group running and mixing

In a realistic BSM scenario the operators in Eq. (1) do not appear in isolation at the hadronic scale. They are generated at some high unknown energy scale and evolved down by QCD (and above the electroweak scale, electroweak) RG running. Two qualitative features of this evolution are important. First, the Wilson coefficients receive multiplicative QCD corrections. For example, the Weinberg operator and the four-quark operators typically receive sizeable multiplicative corrections when evolved from a multi-TeV scale down to a few GeV (Braaten et al. (1990)). In many cases these corrections are of order unity, so they must be taken into account for quantitative work, but they do not completely reshuffle the hierarchy among different sources. Calculations of these corrections have been extended to the two-loop level (Degrassi et al. (2005), de Vries et al. (2020b), Naterop and Stoffer (2026)).

Second, and often more relevant for phenomenology, operators mix under RG evolution. A four-quark operator at a high scale will induce quark EDMs and CEDMs at lower scales through quark-gluon loops. A heavy-quark CEDM generates a Weinberg operator below the heavy-quark threshold. Two-loop Barr-Zee diagrams connect CP-violating Higgs-fermion interactions to fermion EDMs and CEDMs (Barr and Zee (1990), Brod et al. (2024)). The net result is that even a single CP-odd operator at the UV matching scale generates a correlated ensemble of operators at the hadronic scale. The full mixing and matching procedure is discussed in, for example, (Dekens and de Vries (2013); Kley et al. (2022); Choi and Im (2026)). For this reason, EDM analyses at the hadronic, nuclear, atomic, and molecular level should ideally be formulated in terms of the full set of operators in Eq. (1). A global analysis of this type was performed in (Gaul and Berger (2024); Degenkolb et al. (2026)) and illustrates the complementarity of EDM experiments on different systems.

That being said, a useful organizing principle for the various operators is based on their transformation property under the approximate chiral symmetry  $SU(2)_L \times SU(2)_R$  of QCD. As discussed in detail in Sect. 3, these properties determine the form and relative sizes of CP-odd hadronic interactions which, in turn, determines the hierarchy of EDMs. It is therefore useful to group the hadronic operators in Eq. (1) into three distinct classes:

- **Mass-like sources** ( $\bar{\theta}$ , qEDMs, qCEDMs): these transform under  $SU(2)_L \times SU(2)_R$  in the same representation as the quark mass matrix,  $(2_L, \bar{2}_R) \oplus (\bar{2}_L, 2_R)$ . They generate CP-odd pion-nucleon couplings already at leading order in the chiral expansion, and their hadronic consequences closely track those of the  $\bar{\theta}$  term. The  $\bar{\theta}$  term and the isoscalar qCEDM conserve isospin, the isovector qCEDM (with  $\bar{d}_u \neq \bar{d}_d$ ) breaks it.

- **Chiral singlets** (Weinberg operator, chirally invariant four-quark operators): these do not break chiral symmetry at the Lagrangian level. CP-odd pion-nucleon interactions therefore require additional derivatives or quark-mass insertions and are suppressed in the chiral expansion. Short-range nucleon-nucleon interactions play a comparatively larger role for these sources.
- **Tensorial sources** (FQLR operator): these transform as  $(3_L, 3_R)$  under  $SU(2)_L \times SU(2)_R$ . They generate a large isovector pion-nucleon coupling  $\bar{g}_1$  at leading order and a three-pion vertex, leading to a phenomenology that is qualitatively distinct from the  $\bar{\theta}$  term and from chiral singlets.

In addition there are the semi-leptonic operators that fall into their own class. This classification scheme will be used below to organize the discussion of nucleon, nuclear, and atomic/molecular EDMs.

### 3 Chiral effective field theory for CP-odd sources

Below  $\mu \sim 1$  GeV the relevant degrees of freedom are no longer quarks and gluons but pions, nucleons, and heavier hadrons, and photons. The systematic framework for connecting the quark-gluon operators of Sect. 2 to hadronic observables is chiral effective field theory ( $\chi$ EFT), the low-energy EFT of QCD (Weinberg (1979), Gasser and Leutwyler (1984), Weinberg (1990)). Its great advantage is that the structure of the induced CP-violating hadronic interactions, *i.e.* their form and relative sizes, is completely determined by symmetry even though the numerical values of the associated low-energy constants (LECs) require nonperturbative QCD input.  $\chi$ EFT also allows for a systematic calculation of higher-order loop corrections and can incorporate interactions with external currents such as electromagnetism and weak interactions. The construction of the CP-odd chiral Lagrangian in terms of the operators in Eq. (1) has been worked out in (Mereghetti et al. (2010), de Vries et al. (2013), Bsaisou et al. (2015b)). In this section I will explain the method in some detail for the  $\bar{\theta}$  term, which serves as the canonical example, and then summarize the results for the other sources.

#### 3.1 Chiral symmetry and the spurion method

In the absence of electromagnetism and in the limit of vanishing light-quark masses, the QCD Lagrangian for two flavors is invariant under independent  $SU(2)$  rotations of the left- and right-handed quark doublet

$$q_L \rightarrow L q_L, \quad q_R \rightarrow R q_R, \quad L, R \in SU(2)_{L,R}. \quad (11)$$

This chiral symmetry  $G = SU(2)_L \times SU(2)_R$  is spontaneously broken to the diagonal isospin subgroup  $H = SU(2)_V$ , with the three pions as the associated pseudo-Goldstone bosons. They are collected in a unitary matrix

$$U(x) = \exp\left(\frac{i}{F_\pi} \vec{\pi}(x) \cdot \vec{\tau}\right), \quad (12)$$

in terms of the pion triplet  $\vec{\pi}(x)$  and the pion decay constant  $F_\pi \simeq 92.2$  MeV. The matrix transforms under chiral symmetry as  $U \rightarrow LUR^\dagger$ . The key tool for incorporating explicit symmetry breaking is the spurion method. Rather than treating symmetry-breaking terms as perturbations, one formally promotes their coefficients to spurion fields that transform under  $G$  in such a way that the full Lagrangian is chiral invariant. Physical results are recovered by setting the spurion to its actual (symmetry-breaking) value at the end. The power of the method is that it allows one to read off the complete set of allowed operators at any given order in the chiral expansion purely from group theory, without doing any explicit matching calculation. A good example is the quark mass matrix  $M = \text{diag}(m_u, m_d)$ . It breaks chiral symmetry because it couples left- and right-handed quarks. One promotes  $M$  to a spurion transforming as  $M \rightarrow LMR^\dagger$ , so that the combination  $\chi \equiv 2BM$  (with  $B$  related to the quark condensate) can be inserted into the chiral Lagrangian to build invariants. At leading order in the mesonic sector this gives

$$\mathcal{L}_\pi = \frac{F_\pi^2}{4} \text{Tr}[D_\mu U D^\mu U^\dagger] + \frac{F_\pi^2}{4} \text{Tr}[\chi U^\dagger + \chi^\dagger U], \quad (13)$$

where the first term is the pion kinetic energy in terms of covariant derivatives  $D_\mu$  (in this work  $D_\mu$  contains the couplings to photons) and the second term generates the pion mass  $m_\pi^2 = B(m_u + m_d)$ . Note that the pion mass is not predicted as it involves the non-perturbative LEC  $B = \mathcal{O}(\Lambda_\chi)$ , but  $\chi$ EFT does predict a linear dependence on the average quark mass.

Nucleons are introduced as a doublet  $N = (pn)^T$  transforming under the unbroken  $SU(2)_V$ . Because the theory is based on an expansion in  $Q/\Lambda_\chi$  where  $Q \sim m_\pi$  is a low-energy scale and  $\Lambda_\chi \sim 2\pi F_\pi \sim 1$  GeV, virtual nucleon fields inside loop diagrams can lead to factors of  $m_N/\Lambda_\chi = \mathcal{O}(1)$  that break the power counting. This can be avoided by using the fact that nucleons (at least as far as EDM experiments are concerned) are non-relativistic and using a heavy-baryon (HB) description (Jenkins and Manohar (1991)) where the nucleon mass is removed from the nucleon propagator. In such a HB framework it is the spin  $S^\mu = (0, \vec{\sigma}/2)$  and velocity  $v^\mu = (1, \vec{0})$  in the rest frame that appears instead of gamma matrices. In the one-nucleon sector, for our purposes the most relevant Lagrangian in the HB formulation reads

$$\mathcal{L}_{\pi N} = \bar{N} (i v \cdot D + g_A S \cdot u) N + \bar{N} (c_1 \text{Tr} \chi_+ + c_5 \hat{\chi}_+) N. \quad (14)$$

In the first two terms,  $u_\mu = i(u^\dagger \partial_\mu u - u \partial_\mu u^\dagger)$  with  $u^2 = U$ , and  $g_A \simeq 1.27$  the axial coupling gives rise to the leading CP-conserving pion-nucleon interaction. In the last two terms  $\chi_+ = u^\dagger \chi u^\dagger + u \chi^\dagger u$  and  $\hat{\chi}_+ = \chi_+ - \text{Tr}(\chi_+)/2$ . The  $c_1$  and  $c_5$  terms appear at next-to-leading order,

## 6 The theory of electric dipole moments: the view from below

$c_{1,5} = O(\Lambda_\chi^{-1})$ , and describe quark mass contributions to the nucleon mass. In particular

$$\Delta m_N \equiv \frac{(m_n + m_p)}{2} - m_N^0 = -4B(m_u + m_d)c_1, \quad (15)$$

$$\delta m_n \equiv m_n - m_p = -4B(m_d - m_u)c_5, \quad (16)$$

where  $m_N^0$  is the nucleon mass in the chiral limit and it is important to note that  $\delta m_N$  is only the strong part of the nucleon mass splitting and does not include electromagnetic corrections.

### 3.2 The $\bar{\theta}$ term as a worked out example

Let us now apply the spurion method to the  $\bar{\theta}$  term. As shown in Eq. (3), after an axial  $U(1)$  rotation the  $\bar{\theta}$  term becomes an imaginary contribution to the quark mass matrix. This means that the induced CP-odd hadronic interaction can be read from the usual chiral Lagrangian by simply replacing

$$\chi \rightarrow 2B(M + i\bar{\theta}m_\star). \quad (17)$$

Because the  $\bar{\theta}$  term is proportional to the identity matrix in flavor space it leads to isospin-conserving CP-odd interactions. Let's consider the effects on the pion Lagrangian in Eq. (13). The terms proportional to  $\bar{\theta}$  are given by

$$\frac{F_\pi^2}{4}(2iBm_\star)\text{Tr}[U^\dagger - U] = 0, \quad (18)$$

which vanishes exactly. This implies that without insertions of further spurions, the  $\bar{\theta}$  term does not induce CP-violating pionic interactions such as  $\pi^0$  or  $\vec{\pi}^2 \pi^0$ , a direct consequence of isospin conservation.

In the one-nucleon sector we can include  $\bar{\theta}$  in the  $c_1$  and  $c_5$  terms in Eq. (14). A quick calculation shows that the  $c_1$  term is again proportional to  $\text{Tr}(U^\dagger - U) = 0$ . The  $c_5$  term does lead to a non-vanishing interaction

$$\mathcal{L}_{\pi N}(\bar{\theta}) = \bar{g}_0(\bar{\theta})\bar{N}\vec{\tau} \cdot \vec{\pi}N, \quad \bar{g}_0(\bar{\theta}) = -\frac{1}{F_\pi} \frac{m_\star}{m_d - m_u} \delta m_N. \quad (19)$$

This derivation reproduces the famous result of Crewther et al. (1979) and shows how the  $\bar{\theta}$  term induces an isoscalar CP-odd pion-nucleon interaction. In addition, the a priori unknown LEC  $\bar{g}_0(\bar{\theta})$  depends on the strong part of the proton-neutron mass splitting which can be determined by lattice QCD (Aoki et al. (2026)) or dispersive methods (Cottingham (1963)). While this is a tree-level derivation, the connection to the nucleon mass splitting survives loop corrections (de Vries et al. (2015)). Quantitative values of the LECs are discussed in Sect. 3.4.

In similar fashion it is possible to construct CP-odd nucleon-photon and nucleon-nucleon interactions. The former give rise to direct contributions to the nucleon EDM that are necessary to renormalize loop contributions involving  $\bar{g}_0$  (see Sect. 4.1)

$$\mathcal{L}_{N\gamma}(\bar{\theta}) = -2\bar{N}(\bar{d}_0(\bar{\theta}) + \bar{d}_1(\bar{\theta})\tau_3)S^\mu N v^\nu F_{\mu\nu}, \quad (20)$$

where both isospin-breaking and -conserving terms appear because the quark charges break isospin. The nucleon-nucleon terms for the  $\bar{\theta}$  again conserve isospin and, ignoring terms with additional pions, take the form

$$\mathcal{L}_{NN}(\bar{\theta}) = \frac{1}{F_\pi \Lambda_\chi^2} \left[ \bar{C}_1(\bar{\theta})\bar{N}N \partial_\mu(\bar{N}S^\mu N) + \bar{C}_2(\bar{\theta})\bar{N}\tau^a N \partial_\mu(\bar{N}S^\mu \tau^a N) \right], \quad (21)$$

but are expected by naive dimensional analysis (see Sect. 3.4) to be suppressed compared to pion-exchange diagrams involving  $\bar{g}_0(\bar{\theta})$ . The nucleon-nucleon interactions are discussed in more detail in Sect. 4.4.

### 3.3 Other CP-odd sources

The advantage of the spurion method is that it generalizes to the other CP-odd sources. I will go briefly through each class in turn, highlighting the key differences from the  $\bar{\theta}$  case.

**Quark chromo-electric dipole moments.** The qCEDMs transform in the same chiral representation as the quark mass matrix,  $(2_L, \bar{2}_R) \oplus (\bar{2}_L, 2_R)$ , so the spurion analysis proceeds identically to the  $\bar{\theta}$  case. One important difference is that the qCEDMs are not connected through a chiral rotation to quark masses and thus the LECs are not connected to hadron mass spectrum. A second difference is that the qCEDM have an isospin-breaking component for  $\bar{d}_u \neq \bar{d}_d$ . Despite these differences, the construction of the chiral Lagrangian follows that of the  $\bar{\theta}$  term. We introduce a new spurion

$$\tilde{\chi} = 2i\tilde{B} \begin{pmatrix} \bar{d}_u & 0 \\ 0 & \bar{d}_d \end{pmatrix} \quad (22)$$

and replace  $\chi \rightarrow \tilde{\chi}$  and  $c_{1,5} \rightarrow \tilde{c}_{1,5}$  in the chiral Lagrangian. In the pionic sector, the isospin-breaking component,  $\sim (\bar{d}_u - \bar{d}_d)$  leads to the appearance of pion tadpoles  $\pi^0$  and related interactions between an odd number of pions. A tadpole signals an instability of the vacuum and can be eliminated through a procedure called vacuum alignment (Baluni (1979)). One performs an axial quark field redefinition at the quark level to ensure the vacuum is aligned with the true ground state, which eliminates tadpoles at the hadronic level. Alternatively, one can

perform a pion field redefinition at the hadronic level (Mereghetti et al. (2010)), but this must be accompanied by the corresponding nucleon field transformation, or spurious contributions to the nucleon couplings are generated. Either way, for the qCEDM vacuum alignment eliminates pion tadpoles and the associated multi-pion interactions.

Because of isospin breaking, the  $\tilde{c}_1$  term now leads to a non-vanishing structure

$$\mathcal{L}_{\pi N}(\tilde{d}_q) = \tilde{g}_0(\tilde{d}_q) \bar{N} \vec{\tau} \cdot \vec{\pi} N + \tilde{g}_1(\tilde{d}_q) \bar{N} \pi^0 N, \quad \tilde{g}_0(\tilde{d}_q) = -\frac{2\tilde{c}_5 \tilde{B}}{F_\pi} (\tilde{d}_u + \tilde{d}_d), \quad \tilde{g}_1(\tilde{d}_q) = -\frac{4\tilde{c}_1 \tilde{B}}{F_\pi} (\tilde{d}_u - \tilde{d}_d). \quad (23)$$

Nonperturbative calculations are necessary to determine the new LECs  $\tilde{B}$  and  $\tilde{c}_{1,5}$ , but this simple derivations shows that qCEDM generates both  $\tilde{g}_0$  and  $\tilde{g}_1$  at leading order, and  $\tilde{g}_1$  vanishes in the isospin limit  $\tilde{d}_u = \tilde{d}_d$ . The CP-odd nucleon-photon operators are similar to those of the  $\bar{\theta}$  term. The CP-odd nucleon-nucleon interactions are again expected at higher order compared to pion exchange and now include two isospin-breaking terms

$$\mathcal{L}_{NN}(\tilde{d}_q) = \frac{1}{F_\pi \Lambda_\chi^2} \left[ \tilde{C}_1(\tilde{d}_q) \bar{N} N \partial_\mu (\bar{N} S^\mu N) + \tilde{C}_2(\tilde{d}_q) \bar{N} \tau^a N \partial_\mu (\bar{N} S^\mu \tau^a N) + \tilde{C}_3(\tilde{d}_q) \bar{N} N \partial_\mu (\bar{N} S^\mu \tau^3 N) + \tilde{C}_4(\tilde{d}_q) \bar{N} \tau^3 N \partial_\mu (\bar{N} S^\mu N) \right]. \quad (24)$$

**Quark electric dipole moments.** The qEDMs share the same chiral representation as the qCEDMs and hence the same spurion structure. The key physical difference is that the qEDM operator contains an explicit photon field  $F_{\mu\nu}$ . This means that at leading order in the chiral expansion, the qEDM generates the nucleon EDM directly through the short-distance LECs  $\tilde{d}_{0,1}$  in Eq. (20), while the interactions without photons are suppressed by  $\alpha_{em}$ . The qEDM is therefore predominantly a “direct” source of nucleon EDMs rather than a source of CP-odd nuclear forces.

**Weinberg operator and chiral-invariant four-quark operators.** These operators are chiral singlets and the corresponding spurion has a trivial chiral transformation. The key consequence is that no CP-odd pion-nucleon operator can be built at leading order in the chiral expansion. One always needs at least one insertion of the quark-mass spurion  $\chi$  or two extra derivatives and the resulting CP-odd pion-nucleon interactions are therefore suppressed by  $m_\pi^2/\Lambda_\chi^2$  relative to those from the  $\bar{\theta}$  term. This suppression implies that the nucleon EDMs operators and isospin-conserving short-range nucleon-nucleon interactions ( $\tilde{C}_{1,2}(C_W)$ ), which do not require pion-nucleon couplings, play a comparatively larger role than for the CP-odd chiral-breaking sources.

**The four-quark left-right operator.** The FQLR transforms as  $(3_L, 3_R)$  under  $SU(2)_L \times SU(2)_R$ , which is a higher-dimensional representation than the quark mass and a separate construction is necessary. The detailed procedure is spelled out in (de Vries et al. (2013), Bsaisou et al. (2015b)) and shows the appearance of a leading-order tadpole coefficient accompanied by a CP-odd three-pion vertex

$$\mathcal{L}_\pi = m_N \bar{\Delta} \pi_3 \pi^2 + \dots \quad (25)$$

Vacuum alignment again eliminates the tadpole but in this case leaves behind the three-pion interaction. In the pion-nucleon sector the  $\tilde{g}_1$  coupling is expected and significantly larger than  $\tilde{g}_0$ , exactly opposite as for the  $\bar{\theta}$  term. The nucleon-photon and nuclear-nucleon interactions are similar to that of the qCEDM.

**Electron-quark operators.** The hadronization of the electron-quark operators in Eq. (10) is straightforward as the quark bilinears transform in similar fashion as the quark masses under chiral symmetry. Since the electron-structure is not affected, the leading chiral interactions are given by (Dekens et al. (2019))

$$\mathcal{L}_{eN} = \frac{G_F}{\sqrt{2}} \left\{ \bar{e} i \gamma^5 e \bar{N} \left( C_S^{(0)} + C_S^{(1)} \tau^3 \right) N - 4 \bar{e} \sigma_{\mu\nu} e \bar{N} \left( C_T^{(0)} + C_T^{(1)} \tau^3 \right) \gamma^\mu S^\nu N + \bar{e} e \frac{\partial_\mu}{m_N} \left[ N \left( C_P^{(0)} + C_P^{(1)} \tau^3 \right) S^\mu N \right] \right\}. \quad (26)$$

The  $C_S$  structures involve the electron spin and contribute to paramagnetic atomic and molecular EDMs. In fact, in the SM itself, paramagnetic EDMs are dominated by the  $C_S$  contribution (Ema et al. (2022)), while the electron EDM contribution is smaller by several orders of magnitude (Hoozeveen (1990); Yamaguchi and Yamanaka (2020)). The  $C_P$  interaction is suppressed in the non-relativistic limit and will be neglected below.  $C_T$  require a nonzero nuclear spin and mainly contribute to EDMs of diamagnetic atoms such as  $^{199}\text{Hg}$ .

### 3.4 Values of CP-odd low-energy constants

In the above sections, we saw how chiral symmetry is very useful in deriving the form of the low-energy CP-violating hadronic interactions. However, this procedure did not provide information about the values of the accompanying LECs. The success of  $\chi$ EFT depends on LECs to follow an expected scaling, otherwise it is difficult to see how higher-order terms can be treated in perturbation theory. This expected scaling can be derived using a technique called Naive Dimensional Analysis (NDA) introduced in Manohar and Georgi (1984). The NDA rules are most easily summarized by using “reduced” coupling constants (Weinberg (1989)) to match operators at the quark-gluon level to the hadronic level. A coupling constant  $c$  of an interaction of dimension  $D$  involving  $N$  fields has a reduced coupling

$$c^R = \Lambda_\chi^{D-4} (4\pi)^{2-N} c, \quad (27)$$

where  $\Lambda_\chi \sim 1 \text{ GeV}$  is the matching scale. The NDA rule is that the reduced coupling of an operator below  $\Lambda_\chi$  is given by the product of the reduced couplings of the operators above  $\Lambda_\chi$  that induce the operator. For example, take the CP-odd pion-nucleon interaction  $\tilde{g}_0$  with reduced coupling  $(\tilde{g}_0)^R = \tilde{g}_0/(4\pi)$ . If  $\bar{\theta}$  is the underlying CP-violating mechanism than the NDA rules dictate that this equals

## 8 The theory of electric dipole moments: the view from below

$(m_\star \bar{\theta})^R = m_\star \bar{\theta} / \Lambda_\chi$ . Rearranging this gives

$$|\bar{g}_0(\bar{\theta})| = \mathcal{O}\left(\bar{\theta} m_\star \frac{(4\pi)}{\Lambda_\chi}\right) = \mathcal{O}\left(\bar{\theta} m_\star \frac{1}{F_\pi}\right) \simeq 10^{-2} \bar{\theta} \quad (28)$$

To induce  $\bar{g}_1(\bar{\theta})$  an extra source of isospin-breaking is needed which brings in the reduced coupling  $(\delta m_q)^R = (\delta m_q) / \Lambda_\chi$  where  $\delta m_q = m_d - m_u$ , and NDA thus predicts  $|\bar{g}_1(\bar{\theta})| \ll |\bar{g}_0(\bar{\theta})|$ . For  $\bar{\theta}$  it is possible to do better than NDA by using Eq. (19) and the lattice-QCD value of  $\delta m_N$  (Aoki et al. (2026)) to obtain

$$\bar{g}_0(\bar{\theta}) = -(17.2 \pm 2.0) \cdot 10^{-3} \bar{\theta} \quad (29)$$

in good agreement with the NDA estimate. A resonance saturation estimate (Bsaisou et al. (2013)) gives  $\bar{g}_1(\bar{\theta}) \simeq 3 \cdot 10^{-3} \bar{\theta}$  somewhat larger than NDA predicts. The same procedure can be applied to other CP-violating sources. For example, NDA predicts for the qCEDMs

$$\bar{g}_0(\vec{d}_q) = \mathcal{O}\left((\vec{d}_u + \vec{d}_d) \Lambda_\chi\right), \quad \bar{g}_1(\vec{d}_q) = \mathcal{O}\left((\vec{d}_u - \vec{d}_d) \Lambda_\chi\right) \quad (30)$$

in decent agreement with more advanced calculations from QCD sum rules (Pospelov (2002))

$$\bar{g}_0(\vec{d}_q) = (1 \pm 2)(\vec{d}_u + \vec{d}_d) \text{ GeV}, \quad \bar{g}_1(\vec{d}_q) = (7 \pm 5)(\vec{d}_u - \vec{d}_d) \text{ GeV}, \quad (31)$$

considering the large uncertainties. It is crucial to improve the determination of  $\bar{g}_{0,1}$  arising from the qCEDMs and other sources in order to optimally interpret the outcome of EDM experiments.

The above examples show that NDA is a reasonable, but crude, method to determine the (relative) sizes of CP-violating LECs. The NDA estimates for all relevant LECs are shown in Table 1 and can be used as a guide to determine which interactions to include for which source. Entries labelled in dark green appear at leading order in the calculation of nucleon or nuclear CP violation, while the black entries appear at higher order. The orange entries are suppressed according to NDA, but NDA estimates are not always reliable for nucleon-nucleon interactions. This subtlety is discussed in Sect. 4.4. Ideally the NDA estimates are replaced by more accurate calculations in the future. The status of nonperturbative calculations of the nucleon EDMs is briefly discussed in the next section, but also in this case the NDA estimates for  $\vec{d}_{0,1}$  turn out to be reasonable.

For the semi-leptonic interactions the situation is better and NDA is not necessary. The LECs are given by

$$C_S^{(0)} = \frac{\sqrt{2}}{G_F} \frac{2\sigma_{\pi N}}{m_u + m_d} c_S^{(0)}, \quad C_S^{(1)} = \frac{\sqrt{2}}{G_F} \frac{2\delta m_N}{m_d - m_u} c_S^{(1)}, \quad (32)$$

where  $\sigma_{\pi N} = (59.6 \pm 7.4) \text{ MeV}$  (Gupta et al. (2021)) is the pion-nucleon sigma term (related to  $c_1$ ) and  $\delta m_N = (2.5 \pm 0.2) \text{ MeV}$  (Aoki et al. (2026)) the strong proton-neutron mass splitting (related to  $c_5$ ). The tensor couplings are given by

$$C_T^{(0)} = \frac{\sqrt{2}}{G_F} (g_T^u + g_T^d) c_T^{(0)}, \quad C_T^{(1)} = \frac{\sqrt{2}}{G_F} (g_T^u - g_T^d) c_T^{(0)}, \quad (33)$$

where  $g_T^u \simeq -(0.21 \pm 0.01)$  and  $g_T^d \simeq 0.82 \pm 0.03$  are the nucleon tensor charges obtained from lattice QCD (Gupta et al. (2018); Aoki et al. (2026)).

### 3.5 Intermediate summary

The main message of this section is that EDMs of nucleons, nuclei, atoms, and molecules can be expressed in a relatively small number of LECs

$$\{\bar{\Delta}, \bar{g}_0, \bar{g}_1, \vec{d}_0, \vec{d}_1, \bar{C}_i, C_S^{(0,1)}, C_T^{(0,1)}\}. \quad (34)$$

Depending on the CP-violating source under consideration a different subset of these interactions is expected to play a role.

The uncertainties on these LECs vary widely across the different sources and represent one of the main bottlenecks in the interpretation of EDM experiments. For the  $\bar{\theta}$  term, the situation is relatively favorable as  $\bar{g}_0(\bar{\theta})$  is tied to the strong neutron-proton mass splitting determined accurately by lattice QCD. The semi-leptonic LECs  $C_S^{(0,1)}$  and  $C_T^{(0,1)}$  originating from semi-leptonic four-fermion operators are similarly well-determined, being related to  $\sigma_{\pi N}$ ,  $\delta m_N$ , and the nucleon tensor charges, all of which are now precisely known from lattice QCD. For the qCEDMs, the situation is much less satisfactory. The QCD sum rule estimates for  $\bar{g}_{0,1}(\vec{d}_q)$  carry  $\mathcal{O}(100\%)$  uncertainties, and no lattice QCD calculations currently exist. The LECs for the Weinberg operator and chiral-invariant four-quark operators are even less constrained, with only order-of-magnitude estimates available. These uncertainties propagate directly into the interpretation of EDMs limiting the usefulness of EDM measurements in constraining and hopefully identifying these sources. Improving the determination of these LECs through lattice QCD, see Liu (2025) for a recent review, should therefore be a high priority.

A promising path forward is provided by the gradient flow (Lüscher (2010)) which offers a gauge-invariant and systematically improvable renormalization scheme for higher-dimensional CP-odd operators on the lattice. The perturbative matching of the qCEDMs, Weinberg operator, and the CP-odd four-quark operators to the gradient-flow scheme has recently been completed at one loop (Cirigliano et al. (2020); Mereghetti et al. (2022); Bühler and Stoffer (2023)) laying the groundwork for lattice QCD determinations of the hadronic LECs. Preliminary calculations have appeared (Kim et al. (2021); Bhattacharya et al. (2025)), see Shindler (2021) for a more comprehensive discussion.

Source	$\bar{\theta}$	qCEDM	FQLR	qEDM	Weinberg
$\bar{g}_0$	$\bar{\theta}(m_*/F_\pi)$	$\bar{d}_q \Lambda_\chi$	$C_{\text{LR}} m_q F_\pi$	$d_q \Lambda_\chi \frac{\alpha_{\text{em}}}{4\pi}$	$C_W m_q \Lambda_\chi$
$\bar{g}_1/\bar{g}_0$	$m_q/\Lambda_\chi$	1	$\Lambda_\chi/m_q$	1	1
$\bar{\Delta}/\bar{g}_0$	$m_q/\Lambda_\chi$	$m_q/\Lambda_\chi$	$\Lambda_\chi/m_q$	1	$m_q/F_\pi$
$\bar{d}_{0,1}$	$e \bar{\theta}(m_*/\Lambda_\chi^2)$	$e \bar{d}_q (F_\pi/\Lambda_\chi)$	$e C_{\text{LR}} (F_\pi^2/\Lambda_\chi)$	$d_q$	$e C_W F_\pi$
$\bar{C}_{1,2}$	$\bar{\theta}(m_*/F_\pi)$	$\bar{d}_q \Lambda_\chi$	$C_{\text{LR}} m_q F_\pi$	$d_q \Lambda_\chi \frac{\alpha_{\text{em}}}{4\pi}$	$C_W \Lambda_\chi^2$
$\bar{C}_{3,4}/\bar{C}_{1,2}$	$m_q/\Lambda_\chi$	1	$\Lambda_\chi/m_q$	1	$m_q/\Lambda_\chi$

Table 1: NDA estimates of the CP-odd hadronic LECs for each hadronic source of CP violation. Entries in **dark green** indicate leading-order contributions, while entries in **orange** denote contributions that are subleading by NDA but could possibly be enhanced through renormalization, see Sect. 4.4. Uncolored entries are suppressed by at least one power of  $m_q/\Lambda_\chi$  relative to the leading contribution in the same column. Here  $m_* = m_u m_d/(m_u + m_d)$  is the reduced quark mass,  $m_q$  denotes the quark mass,  $\Lambda_\chi \sim 1$  GeV is the chiral symmetry breaking scale, and  $F_\pi \simeq 92.2$  MeV is the pion decay constant.

## 4 Electric dipole moments of nucleons and nuclei

### 4.1 Nucleon electric dipole moments and Schiff moments

The EDMs of the neutron and proton provide the most direct measurements of hadronic CP violation without requiring further atomic/molecular calculations of screening or enhancement factors. That being said, the computation of nucleon EDMs in terms of the underlying CP-odd mechanism is not an easy task. Various approaches exist in the literature including quark models (Dib et al. (2006); Yamanaka and Hiyama (2021)), QCD sum rules (Pospelov and Ritz (1999); Hisano et al. (2012); Haisch and Hala (2019)),  $\chi$ PT (Borasoy (2000); Hockings and van Kolck (2005); de Vries et al. (2011c)), holography (Hong et al. (2007); Bartolini et al. (2017)), and lattice QCD. Most effort has focused on the QCD  $\bar{\theta}$  term and the quark EDMs, while much less is known about the quark chromo-EDMs, Weinberg operator, or four-quark interactions.

Chiral techniques are useful when the nucleon EDMs depend on a chiral logarithm  $\sim \log m_\pi$  which is enhanced in the chiral limit. However, these contributions are typically divergent and thus require short-distance (here short-distance means from distances shorter-than-pion-range) contributions that renormalize the EDM.  $\chi$ PT does not predict the values of these short-distance contributions leading to an increase in theoretical uncertainty. One-loop diagrams involving  $\bar{g}_0$  and  $\bar{g}_1$  have been computed up to next-to-leading order (Crewther et al. (1979); Ottnad et al. (2010); Mereghetti et al. (2011)) and give

$$\begin{aligned}
 d_n &= \bar{d}_0(\mu) - \bar{d}_1(\mu) - \frac{e g_A \bar{g}_0}{8\pi^2 F_\pi} \left( \ln \frac{m_\pi^2}{\mu^2} - \frac{\pi m_\pi}{2m_N} \right), \\
 d_p &= \bar{d}_0(\mu) + \bar{d}_1(\mu) + \frac{e g_A}{8\pi^2 F_\pi} \left[ \bar{g}_0 \left( \ln \frac{m_\pi^2}{\mu^2} - \frac{2\pi m_\pi}{m_N} \right) - \bar{g}_1 \frac{\pi m_\pi}{2m_N} \right].
 \end{aligned} \tag{35}$$

The short-distance contributions  $\bar{d}_0 \mp \bar{d}_1$  have a scale dependence in order to absorb the scale dependence of the chiral logarithms. At this order, the neutron EDM does not depend on  $\bar{g}_1$  and the first dependence appears at next-to-next-to-leading order (Seng et al. (2014)). Setting  $\mu = m_N$  and assuming the chiral logarithm to dominate the short-distance pieces gives

$$d_n(\bar{\theta}) \simeq -d_p(\bar{\theta}) \simeq 10^{-3} \bar{\theta} e \text{ fm}, \tag{36}$$

in good agreement with results from QCD sum rules (Pospelov and Ritz (1999)). More recently lattice QCD (Dragos et al. (2021); Liang et al. (2023)) has been applied to compute the nucleon EDMs, see Liu (2025) for a review, giving

$$d_n(\bar{\theta}) = -(1.48 \pm 0.34) \cdot 10^{-3} \bar{\theta} e \text{ fm}, \quad d_p(\bar{\theta}) = (3.8 \pm 1.4) \cdot 10^{-3} \bar{\theta} e \text{ fm}. \tag{37}$$

For the quark chromo-EDM the pion loops are also expected to be dominant but the values of  $\bar{g}_{0,1}$  are less well known. QCD sum rules results are obtained in (Pospelov and Ritz (2001); Hisano et al. (2012)).

For quark EDMs, the pion-loops are subleading and chiral techniques are not useful. In this case, lattice QCD calculations of nucleon tensor charges have become very accurate (Gupta et al. (2018), Aoki et al. (2026)) and

$$d_n(d_q) = g_T^u d_u + g_T^d d_d, \quad d_p(d_q) = g_T^d d_u + g_T^u d_d, \tag{38}$$

where the tensor charges are given in Sect. 3.4. The role of the strange quark EDM is less clear. For chiral-symmetry-conserving sources such as the Weinberg operator, the pion loops are expected to be subleading as well. In this case only estimates exist based on QCD sum rules (Demir et al. (2003); Haisch and Hala (2019)) and quark models (Yamanaka and Hiyama (2021)) giving

$$d_n(C_W) \simeq (30 \pm 20) \text{ MeV } e C_W, \tag{39}$$

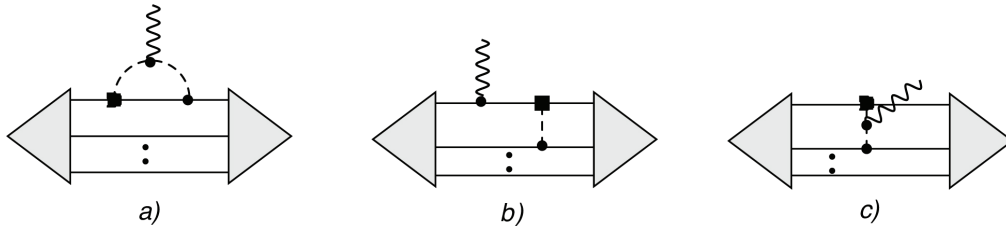


Fig. 2: Three contributions to a nuclear EDM described in the text. Solid, wavy, and dashed lines denote nucleons, photons, and pions, respectively. The triangle denotes the nuclear wavefunction and the dots denote the  $A - 2$  nucleon propagators. The black square denotes the CP-odd pion-nucleon vertex  $\bar{g}_0$  while the black circles denote CP-conserving interactions.

where the uncertainty is chosen to span the range of predictions. The proton EDM comes with a similar matrix element but with opposite sign (Haisch and Hala (2019)). These values are consistent with the NDA expectation of Table 1.

While chiral techniques are of limited use for nucleon EDMs, the momentum dependence encoded in the nucleon electric dipole form factor (EDFF) can be predicted. The nucleon EDFF can be decomposed as

$$F_{n,p}(Q^2) = d_{n,p} - S'_{n,p}Q^2 + H_{n,p}(Q^2), \quad (40)$$

where  $Q^2 = -q^2 > 0$  indicates the momentum transfer from the photon with outgoing four-momentum  $q^\mu$ . For chiral-breaking CP-odd sources, the nucleon Schiff moments,  $S'_{n,p}$  (the prime indicates that this is not the full nucleon Schiff moment as discussed in Sect. 5), are dominated by the pion cloud (Thomas (1995)) and, up to small isospin-breaking corrections, isovector in nature (Mereghetti et al. (2011))

$$S'_n = -S'_p = \frac{e g_A \bar{g}_0}{48\pi^2 F_\pi m_\pi^2} \left(1 - \frac{5\pi m_\pi}{4m_N}\right). \quad (41)$$

The EDFF shape functions encoded in  $H_{n,p}$  start at  $\mathcal{O}(Q^4)$  and are also completely specified (de Vries et al. (2011c)). They can be used to guide lattice QCD extrapolations in the  $Q^2 \rightarrow 0$  limit. For the qEDM and chiral-invariant sources, the nucleon Schiff moments are suppressed and come with undetermined low-energy constants. This implies that the ratio of nucleon Schiff moments to nucleon EDMs is indicative of the underlying source of CP violation. Unfortunately nucleon Schiff moments are not directly measured and probing this ratio is difficult.

## 4.2 Electric dipole moments of atomic nuclei

After the nucleon EDMs, the next level in complexity is to consider nuclear EDMs. Up to very recently, no nuclear EDMs were directly measured but this changed with the first limit on the deuteron EDM set by the JEDI collaboration (Andres et al. (2026)). By storing the deuteron ( $D$ ) in an electromagnetic storage ring and tracking the tilt of the spin axis with respect to the ring plane, it was possible to constrain

$$d_D < 2.5 \cdot 10^{-17} \text{ e cm}. \quad (42)$$

While this limit is 9 orders away from the direct neutron EDM limit, it provides a proof-of-principle measurement and motivates the construction of future dedicated experiments. Such storage rings have been proposed for protons, light nuclei, light ions, and muons (Alexander et al. (2022), Adelman et al. (2025), Dutsov et al. (2025)).

From the theoretical point of view, the main difference between nuclear and nucleon EDMs is the contribution from multi-nucleon CP-odd mechanisms. In addition to the single nucleon EDM contributions, there are novel contributions from multi-nucleon CP-odd electromagnetic currents and from the interplay of CP-odd nuclear forces and CP-conserving currents. Because nuclear calculations are difficult (even for the deuteron) it is useful to use power counting to assess the (relative) sizes of the various contributions.

Let us consider three contributions shown in Fig. 2 involving the CP-odd pion-nucleon vertex  $\bar{g}_0$ . Diagram 2a) represents a one-loop contribution to the nucleon EDM (see Eq. (35)) which then enters the nuclear system, diagram 2b) represents an insertion of a CP-odd pion exchange involving  $\bar{g}_0$  and  $g_A$  and an insertion of the proton charge, while finally diagram 2c) is a contribution from a CP-odd pion-in-flight current involving one  $\bar{g}_0$  vertex and one strong CP-conserving pion-nucleon vertex  $\sim g_A$ .

We now briefly discuss the power counting of these diagrams. In heavy-baryon  $\chi$ PT, in loop diagrams involving a single nucleon field, it is always possible to avoid the nucleon pole when doing the virtual  $k^0$  energy integration. In such diagrams, the pion and nucleon propagators count respectively as  $1/Q^2$  and  $1/Q$  where  $Q \sim m_\pi$ . In addition, each loop integration counts as  $Q^4/(4\pi)^2$ . Weinberg noticed that in two-nucleon diagrams the nucleon poles cannot always be avoided leading to a ‘pinch’ singularity (Weinberg (1990)) and picking up energies  $\sim Q^2/m_N$  instead. This enhances each nucleon propagator to count as  $m_N/Q^2$  instead of  $1/Q$ . The integration measure now counts as  $Q^5/(4\pi m_N)$  where the extra  $4\pi$  arises from the loop topologies (van Kolck (2020a)). Using these rules we can now quickly estimate the contributions from the 3 diagrams in Fig. 2. We normalize the diagrams by omitting the common  $A - 1$  loop integrations and  $A + 1$  nucleon propagators that contribute to all diagrams. Diagram a) then simply contributes

$$D_a = \mathcal{O}(Q d_{n,p}) = \mathcal{O}\left(\frac{e g_A \bar{g}_0}{(4\pi)^2}\right), \quad (43)$$

where the  $Q$  arises from the derivative in the nucleon EDM vertex. The second equality uses  $Q \sim F_\pi$  and holds for sources where the nucleon EDMs get leading contributions from pion loops. Now consider diagram b) which contains one extra loop,  $Q^5/(4\pi m_N)$ , two extra nucleon propagators,  $m_N^2/Q^4$ , one pion propagator,  $1/Q^2$ , and a combination of pion-nucleon vertices  $Qg_A\bar{g}_0/F_\pi \sim g_A\bar{g}_0$ . Combining the factors predicts

$$D_b = O\left(e\frac{g_A\bar{g}_0m_N}{4\pi Q}\right). \quad (44)$$

Using  $4\pi Q \sim m_N$  shows that diagram b), arising from CP-odd nuclear forces, is enhanced by  $(4\pi)^2 \sim \Lambda_\chi^2/Q^2$  with respect to the nucleon EDM contributions. Such an enhancement was already noted a long time ago in Flambaum et al. (1984).

Contribution from CP-odd two-nucleon currents are bit trickier to count. The topology of diagram c) involves a pion-photon vertex which, in order to generate an EDM, contributes a pion energy  $q^0 \sim Q^2/m_N$ . Taking this suppression into account leads to

$$D_c = O\left(\frac{e g_A \bar{g}_0}{(4\pi)^2}\right), \quad (45)$$

at the same order as the nucleon EDMs. Note that at this order several other CP-odd currents appear (de Vries et al. (2011a)).

Of course, power counting only provides a guide and explicit calculations are necessary to confirm the above results, but the initial conclusion is that EDMs (and Schiff moments) of nuclear systems are dominated by CP-odd nuclear forces that cause nuclear ground states to obtain a small admixture of opposite parity states. The CP-conserving electromagnetic current connects the parity-admixed states back into the ground state. Schematically, the calculation involves calculating the nuclear ground state wave function,  $\Psi_A$ , by solving a Schrödinger equation involving a CP-even nuclear Hamiltonian,  $\mathcal{H}_{CP}$ , and then perturbing this wave function with a CP-odd nuclear potential,  $V_{CP}$ , to obtain the parity-admixed wave function  $\tilde{\Psi}_A$ :

$$\begin{aligned} (E - \mathcal{H}_{CP})|\Psi_A\rangle &= 0, \\ (E - \mathcal{H}_{CP})|\tilde{\Psi}_A\rangle &= V_{CP}|\Psi_A\rangle. \end{aligned} \quad (46)$$

The EDM is then proportional to the transition matrix element

$$d_A \sim \langle \Psi_A | J_{CP} | \tilde{\Psi}_A \rangle, \quad (47)$$

where  $J_{CP}$  is the CP-conserving current which, at leading order, simply arises from minimal coupling to the proton charge but gets higher-order corrections, for example, from photons coupling to pions-in-flight.

### 4.3 The CP-violating nucleon-nucleon potential

The above discussion shows that the calculation of nuclear EDMs and Schiff moments requires the CP-odd nucleon-nucleon (or multi-nucleon potential). Historically this potential was derived using one-meson-exchange models involving a combination of CP-even and CP-odd meson-nucleon interactions. The CP-violating potential can also be calculated using  $\chi$ EFT which has the main advantage that higher-order corrections, not necessarily described by one-meson exchange, can be computed systematically. A detailed review of the derivation of CP-violating nuclear potentials is given by de Vries et al. (2020a), and here I discuss the main features.

CP-violating nuclear forces can be computed from the interactions in Sect. 3. The pion-nucleon, three-pion vertices, and short-range interactions contribute to nucleon-nucleon interactions through diagrams depicted in Fig. 3. The most important diagrams are the one-pion-exchange (OPE) diagrams, Fig. 3a), which lead to

$$V_{\mathcal{CP}}^{\text{OPE}} = i\frac{g_A\bar{g}_0}{2F_\pi}(\vec{\tau}_1 \cdot \vec{\tau}_2)\frac{\vec{k} \cdot (\vec{\sigma}_1 - \vec{\sigma}_2)}{\vec{k}^2 + m_\pi^2} + i\frac{g_A\bar{g}_1}{4F_\pi}\left[(\tau_1^3 + \tau_2^3)\frac{\vec{k} \cdot (\vec{\sigma}_1 - \vec{\sigma}_2)}{\vec{k}^2 + m_\pi^2} + (\tau_1^3 - \tau_2^3)\frac{\vec{k} \cdot (\vec{\sigma}_1 + \vec{\sigma}_2)}{\vec{k}^2 + m_\pi^2}\right], \quad (48)$$

where  $\vec{\tau}_{1,2}$  and  $\vec{\sigma}_{1,2}$  are, respectively, the isospin and spin of the involved nucleons, and  $\vec{k} = \vec{p}'_1 - \vec{p}_1$  is the momentum transfer between the nucleons. The tree-level contributions are obtained from using standard Feynman rules and neglecting the virtual pion energies  $k_0 \ll |\vec{k}|$  as indicated by the power counting rules in the previous section. The  $\bar{g}_0$  OPE potential conserves isospin and leads to  $^1S_0$ - $^3P_0$  mixing with equal strengths for  $nn$ ,  $pp$ , and  $np$  (here  $n$  and  $p$  denote neutron and proton), and to  $^3S_1$ - $^1P_1$  mixing for  $np$ . The first term in the  $\bar{g}_1$  OPE potential however violates isospin and leads to  $^1S_0$ - $^3P_0$  mixing for  $pp$  and  $nn$  (with opposite sign) but not for  $np$ . The second term proportional to  $\bar{g}_1$  changes total isospin by one unit and leads to  $^3S_1$ - $^3P_1$  for  $np$  systems. CP-odd two-pion exchange potentials, Fig. 3b), appear at next-to-next-to-leading order (and beyond) (Maekawa et al. (2011)) and are not negligible at least for EDMs of light nuclei (Gnech and Viviani (2020)). The role of  $\Delta$ -baryons has been investigated showing that no new CP-violating LECs are required (Gandor et al. (2024)).

The three-pion vertex in Eq. (25) contributes at one loop, Fig. 3c), to the same spin-isospin structure as  $\bar{g}_1$  but with more complicated dependence on the momentum transfer  $\vec{k}^2$  (de Vries et al. (2013))

$$V_{\mathcal{CP}}^{\text{OPE},\Delta} = -i\frac{15g_A^3m_\pi m_N \bar{\Delta}}{128\pi F_\pi^3}\left[(\tau_1^3 + \tau_2^3)\frac{\vec{k} \cdot (\vec{\sigma}_1 - \vec{\sigma}_2)}{\vec{k}^2 + m_\pi^2} + (\tau_1^3 - \tau_2^3)\frac{\vec{k} \cdot (\vec{\sigma}_1 + \vec{\sigma}_2)}{\vec{k}^2 + m_\pi^2}\right]\left[1 + f\left(\frac{|\vec{k}|}{2m_\pi}\right)\right], \quad (49)$$

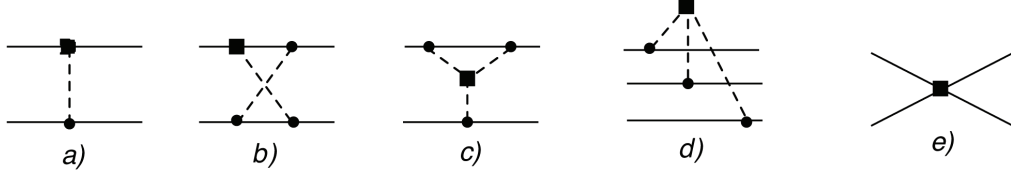


Fig. 3: Several diagrams contributing to the CP-odd nucleon-nucleon potential. Solid and dashed lines denote nucleons and pion, respectively. Black squares (black circles) are CP-odd (CP-even) interactions.

where

$$f(x) = \frac{1 + 2x^2}{3x} \arctan(x) - \frac{1}{3}. \quad (50)$$

The part independent of  $f(x)$  in Eq. (49) provides a renormalization of  $\bar{g}_1$  (de Vries et al. (2013)). Higher-order one-loop diagrams have been computed by Gnech and Viviani (2020). The three-pion vertex also leads to a CP-odd three-nucleon potential, Fig. 3d), at tree level

$$V_{\mathcal{CP}}^{\text{NNN}} = -i \frac{g_A^3 m_N \bar{\Delta}}{4F_\pi^2} \left( \vec{\tau}_1 \cdot \vec{\tau}_2 \tau_3^3 + \vec{\tau}_1 \cdot \vec{\tau}_3 \tau_2^3 + \vec{\tau}_2 \cdot \vec{\tau}_3 \tau_1^3 \right) \frac{(\vec{k}_1 \cdot \vec{\sigma}_1)(\vec{k}_2 \cdot \vec{\sigma}_2)(\vec{k}_3 \cdot \vec{\sigma}_3)}{(\vec{k}_1^2 + m_\pi^2)(\vec{k}_2^2 + m_\pi^2)(\vec{k}_3^2 + m_\pi^2)}, \quad (51)$$

where  $\vec{k}_i$  is the three-momentum that flows to each nucleon.

The CP-violating nucleon-nucleon interactions, Fig. 3e), give rise to short-range potentials

$$V_{\mathcal{CP}}^{\text{short}} = \frac{1}{F_\pi \Lambda_\chi^2} \left[ i \bar{C}_1 \vec{k} \cdot (\vec{\sigma}_1 - \vec{\sigma}_2) + i \bar{C}_2 \vec{k} \cdot (\vec{\sigma}_1 - \vec{\sigma}_2) \vec{\tau}_1 \cdot \vec{\tau}_2 + i \frac{\bar{C}_3 + \bar{C}_4}{2} \vec{k} \cdot (\vec{\sigma}_1 - \vec{\sigma}_2) (\tau_1^3 + \tau_2^3) + i \frac{\bar{C}_3 - \bar{C}_4}{2} \vec{k} \cdot (\vec{\sigma}_1 + \vec{\sigma}_2) (\tau_1^3 - \tau_2^3) \right]. \quad (52)$$

Which of the above terms are relevant depends on the underlying CP-violating source, see Table 1. For the  $\bar{\theta}$  term and qCEDM the OPE potentials proportional to, respectively,  $\bar{g}_0$  and  $\bar{g}_{0,1}$  are expected to dominate nuclear EDMs. For the FQLR  $\bar{g}_1$  and the induced terms by  $\bar{\Delta}$  appear at leading order. For the Weinberg operator, on the other hand, we expect relevant contributions from both OPE as well as the short-range interactions  $\bar{C}_{1,2}$ .

#### 4.4 Renormalization of CP-odd nuclear forces and short-distance nucleon-nucleon interactions

The dominant CP-odd nuclear forces are usually assumed to arise from long-range one-pion exchange (OPE) generated by CP-odd pion–nucleon couplings. For chiral-symmetry-breaking sources of CP violation such as the  $\bar{\theta}$  term and qCEDMs, power counting combined with NDA then places purely short-distance CP-odd  $NN$  operators at next-to-next-to-leading order (see Table 1), suggesting that nuclear EDMs are largely controlled by a small set of long-range couplings. The analysis in de Vries et al. (2021b) revisited this assumption by enforcing renormalization of CP-odd amplitudes in channels where the CP-even tensor nucleon-nucleon ( $NN$ ) force is strong and attractive. In the  ${}^3P_0$  partial wave the attractive tensor OPE is singular (Nogga et al. (2005)) and this leads to  ${}^3P_0$  phase shifts that are very sensitive to the applied regulator. Nogga et al. (2005) suggested to promote  $P$ -wave nucleon-nucleon interactions to leading order, going against NDA expectations. A much more detailed discussion can be found in van Kolck (2020b).

After renormalizing the CP-conserving interactions we add the CP-odd potential as a perturbation. When the long-range CP-odd OPE potential involving  $\bar{g}_0$  or  $\bar{g}_1$  is iterated together with the strong  $NN$  interaction, the resulting CP-odd mixing amplitude for  ${}^1S_0$ – ${}^3P_0$  transitions shows a strong and oscillatory dependence on the ultraviolet regulator. Since observable CP-odd mixing angles must be regulator independent, this behaviour signals that CP-violating OPE alone is not sufficient: a short-distance counterterm is required to absorb the divergence. The required counterterms have the structure of a local CP-odd  $NN$  interaction that induces  ${}^1S_0$ – ${}^3P_0$  transitions and are described by the combinations  $\bar{C}_1 + \bar{C}_2$  (for the  $\bar{g}_0$  OPE) and  $\bar{C}_3 + \bar{C}_4$  (for the  $\bar{g}_1$  OPE). NDA would assign these short-range interactions to subleading order, but the renormalization analysis shows that its coefficient is enhanced and must be counted as leading order. This is signaled by the orange entries in Table 1. A similar enhancement of short-distance  $NN$  physics occurs in the  $\chi$ EFT description of neutrinoless double beta decay (Cirigliano et al. (2018)). Once the short-distance LECs are promoted to leading order, the theory can be renormalized and the  ${}^1S_0$ – ${}^3P_0$  mixing amplitude becomes regulator independent for a wide range of cutoffs. Other CP-odd mixing, such as those for  ${}^3S_1$ – ${}^1P_1$  and  ${}^3S_1$ – ${}^3P_1$ , are already stable and remain dominated by long-range OPE.

This has direct implications for EDM phenomenology. Many nuclear EDMs receive important contributions from  ${}^1S_0$ – ${}^3P_0$  transitions in proton–neutron, proton–proton, and neutron–neutron pairs, so their values generally depend on the short-distance LEC  $\bar{C}_1 + \bar{C}_2$  and  $\bar{C}_3 + \bar{C}_4$  at the same order as on the long-range  $\bar{g}_{0,1}$  terms. In other words, for these systems one cannot reliably predict EDMs (or their ratios) in terms of the underlying QCD  $\bar{\theta}$  angle or other CP-odd sources using pion-exchange interactions alone. Consequently, nuclear EDMs and Schiff moments of light and heavy nuclei such as  ${}^3\text{He}$ ,  ${}^{199}\text{Hg}$ , and  ${}^{225}\text{Ra}$ , which are sensitive to  ${}^1S_0$ – ${}^3P_0$  mixing, would receive contribution from both long-range pions and LO short-range CP-odd  $NN$  contact terms. An important exception is the deuteron EDM, which, as discussed below, is dominated by  ${}^3S_1$ – ${}^3P_1$  mixing.

A central challenge is to determine the short-range LECs in order to assess whether they really play an important role. Lattice QCD calculations of  $NN$  scattering in a nonzero  $\bar{\theta}$  (or other CPV source) background could in principle allow a direct matching of chiral EFT to QCD, though this is technically demanding. Second, for the  $\bar{\theta}$  term, chiral symmetry relates the CP-odd contact interaction to CP-even but

isospin-breaking  $NN\pi$  operators that contribute to charge-symmetry breaking in pion production reactions such as  $NN \rightarrow d\pi$  (van Kolck et al. (2000)) and  $dd \rightarrow \alpha\pi^0$  (Nogga et al. (2006)). Precision data on these processes, analyzed within renormalized chiral EFT, may thus provide an indirect handle on the short-distance CP-odd  $NN$  couplings. Right now such studies have not been carried out, leaving the role of short-range CP-odd nuclear forces an open question.

#### 4.5 Electric dipole moments of light nuclei

We are now ready to discuss explicit computation of nuclear EDMs. The most interesting system is the deuteron which is relatively easy to describe and has been constrained experimentally (Andres et al. (2026)). The deuteron EDM has been computed with various theoretical methods using phenomenological meson-exchange CP-conserving and CP-violating potentials (Afnan and Gibson (2010); Liu and Timmermans (2004)) to  $\chi$ EFT calculations (de Vries et al. (2011a); Bsaisou et al. (2015a); Gnech and Viviani (2020)) to holographic methods (Bartolini et al. (2020)). To reasonable accuracy the deuteron EDM can be calculated analytically in  $\chi$ PT under the assumption that CP-conserving pion exchange is treated perturbatively (de Vries et al. (2011b)), a decent approximation in a loosely bound nuclear system such as the deuteron. In this approximation, the leading CP-conserving nucleon-nucleon potential is a contact potential leading to a zero-range deuteron wave function and, at leading order, the EDM results agree with Khriplovich and Korokin (2000). In this approach, the deuteron EDM is given by

$$d_D = d_n + d_p + \frac{eg_A \bar{g}_1}{12\pi F_\pi} \frac{m_N}{m_\pi} \frac{1 + \xi}{(1 + 2\xi)^2} \simeq d_n + d_p + 0.23 \bar{g}_1 e \text{ fm}. \quad (53)$$

Here  $\xi = \gamma/m_\pi \simeq 0.33$  where  $\gamma = \sqrt{m_N E_b} \simeq 45$  MeV in terms of the deuteron binding energy  $E_b = 2.2$  MeV. The analytical result explicitly confirms the power-counting expectation in Eq. (44). The deuteron spin-isospin properties (the ground state is mainly  ${}^3S_1$  with a small  ${}^3D_1$  admixture) ensure that  $\bar{g}_0$  and  $\bar{C}_{1,2}$  do not contribute to the deuteron EDM at this order. Isospin-breaking corrections appear at higher order but are very small (de Vries et al. (2011a)). The deuteron EDM results have been confirmed with more advanced numerical calculations using phenomenological and  $\chi$ EFT potentials to describe the deuteron wave function (Bsaisou et al. (2015a), Gnech and Viviani (2020)). This slightly changes the numerical coefficients in front of the CP-odd LECs

$$d_D = 0.94(d_n + d_p) + [0.19 \bar{g}_1 - 0.30 \bar{\Delta}] e \text{ fm}, \quad (54)$$

where the uncertainty on the  $\bar{g}_1$  and  $\bar{\Delta}$  coefficients is around 20% based on regulator variations in the numerical calculations and missing higher-order corrections. The three-pion vertex  $\sim \bar{\Delta}$  mainly contributes by effectively renormalizing  $\bar{g}_1$  with roughly 10% contributions from the  $f(\vec{k}/(2m_\pi))$  part in Eq. (49).

While not directly targeted in experimental storage rings, although plans do exist (Alexander et al. (2022); Dutsov et al. (2025)), it is interesting to slowly increase the number of nucleons. The  ${}^3\text{He}$  and  ${}^3\text{H}$  EDMs have been calculated with one-meson-exchange potentials (Stetcu et al. (2008); Song et al. (2013)), pionless EFT (Yang et al. (2021)), and  $\chi$ EFT (de Vries et al. (2011a); Bsaisou et al. (2015a); Gnech and Viviani (2020)). Compared to the deuteron, the main difference is the sensitivity to  $\bar{g}_0$  and  $\bar{C}_i$  and to the CP-odd three-nucleon force induced by the three-pion interaction. Using the most recent results from Gnech and Viviani (2020), the  ${}^3\text{He}$  EDM is

$$\begin{aligned} d_{{}^3\text{He}} = & 0.91 d_n - 0.033 d_p + [(0.056 \bar{g}_0 + 0.16 \bar{g}_1) + (-0.20 - 0.18) \bar{\Delta}] e \text{ fm} \\ & + [0.002(\bar{C}_1 + \bar{C}_2) - 0.008(\bar{C}_1 - \bar{C}_2) - 0.01(\bar{C}_3 - \bar{C}_4)] e \text{ fm}. \end{aligned} \quad (55)$$

The  ${}^3\text{H}$  EDM is obtained by swapping  $d_n \leftrightarrow d_p$  and setting  $\bar{g}_0 \rightarrow -\bar{g}_0$  and  $\bar{C}_{1,2} \rightarrow -\bar{C}_{1,2}$ . The  ${}^3\text{He}$  EDM is essentially the neutron EDM combined with contributions from the CP-odd potential. Compared to the deuteron there is a comparable sensitivity to  $\bar{g}_1$  and a somewhat smaller dependence on  $\bar{g}_0$ . The contributions from  $\bar{\Delta}$  is split into a loop-induced piece from Eq. (49) and higher-order corrections ( $-0.2$ ) and a contribution ( $-0.18$ ) from the CP-odd three nucleon-force in Eq. (51). The three-nucleon contribution was also computed by Bsaisou et al. (2015a) and found to be smaller by an order of magnitude. The reason for the discrepancy with Gnech and Viviani (2020) is not clear and motivates an independent calculation. The second line of Eq. (55) contains contributions from the short-distance CP-odd nucleon-nucleon interactions. By NDA these are expected to small for sources like  $\bar{\theta}$ , qCEDMs, and the FQLR but for chiral-invariant sources  $\bar{C}_{1,2}$  are expected to give relevant contributions. I have added a contribution from  $\bar{C}_3 - \bar{C}_4$  which, although expected to be small by NDA, might have to be promoted to leading order to ensure proper renormalization as discussed in Sect. 4.4.

Calculations have been extended to larger (but still light) nuclei in various approaches. In a series of works, the  $\alpha$  cluster model was applied to compute the EDMs of nuclei such as  ${}^6\text{Li}$ ,  ${}^9\text{Be}$ , and  ${}^{13}\text{C}$  (Yamanaka and Hiyama (2015); Yamanaka (2017); Yamanaka et al. (2019)). The model is based on the observation that the  $\alpha$  cluster is stable and larger systems can be described as collections of  $\alpha$  particles and individual nucleons, simplifying the many-body problem (Yamada et al. (2012)). For example,  ${}^6\text{Li}$  can be seen as a  $\alpha$ - $n$ - $p$  system where the  $n$ - $p$  system is well described by a deuteron cluster. The  ${}^6\text{Li}$  EDM is then arising approximately from the deuteron EDM in addition to contributions from a  $\alpha$ -nucleon CP-odd potential. The latter potential is obtained by folding the CP-odd nucleon-nucleon potential with an ansatz for the nucleon density in the  $\alpha$  cluster. The EDM is calculated as

$$d_{{}^6\text{Li}} = 0.88(d_n + d_p) + 0.28 \bar{g}_1 e \text{ fm} + \dots, \quad (56)$$

where only the nucleon EDM and pion-exchange pieces are kept. The  $\bar{g}_1$  coefficient is 50% larger than that of the deuteron due to the addition  $\alpha$ -nucleon CP-odd force. More recently, a larger set of light nuclear EDMs, up to  ${}^{19}\text{F}$ , were computed in the no-core shell model using  $\chi$ EFT CP-conserving and CP-odd one-meson-exchange potentials (Froese and Navratil (2021)). No systems with large enhancements

over the deuteron were identified.

It is now possible to see if nuclear EDMs are indeed enhanced over nucleon EDMs. Let's take the deuteron EDM as an example and consider the qCEDM as the CP-violating source. From the NDA estimates in Table 1, we expect  $(d_n + d_p) \sim e\tilde{d}_q(F_\pi/\Lambda_\chi)$  while  $0.19 \bar{g}_1 e \text{ fm} \simeq e\tilde{d}_q$ . While we used NDA estimates for the LECs a similar conclusion is reached when using QCD sum rules. So indeed, the nuclear force contribution is expected to dominate over the sum of the nucleon EDMs by a factor  $\Lambda_\chi/F_\pi$  if the qCEDM is the underlying mechanism. If on the other hand, the qEDM is the dominant source we would expect the deuteron EDM to be approximated by the sum of the nucleon EDMs. The fact that different sources of CP violation leads to different ratios of nuclear-to-nucleon EDMs implies that the source can be unraveled from measurements on different systems (Dekens et al. (2014)).

## 5 Diamagnetic electric dipole moments and Schiff's theorem

While EDMs of light nuclei are interesting from a theoretical point of view, at present the experimental sensitivities are not impressive. Atoms and molecules are much easier to manipulate in the laboratory and resulting EDM limits on these neutral systems are very strong. For example, the limit on the EDM of the diamagnetic atom (with closed electron shells)  $d_{199\text{Hg}} < 7.4 \cdot 10^{-30} e \text{ cm}$  (Graner et al. (2016)). While this limit is 2500 times stronger than that on the neutron EDM, a direct comparison is misleading because of electron screening effects that suppress contributions from nuclear CP violation to diamagnetic atomic EDMs. This electron screening, often called Schiff shielding (Schiff (1963)), can classically be understood from the fact that a neutral bound system composed of charged constituents does not move in presence of an external electric field. That is, the constituents rearrange in such a way that the center of mass feels a vanishing electric field. This theorem can be made exact in quantum mechanics for neutral systems of non-relativistic point particles, see Engel et al. (2000) for a pedagogical derivation.

In diamagnetic systems Schiff screening is (somewhat) avoided by the fact that nuclei are extensive objects and this leads to nonzero atomic EDMs. The important quantity, discussed below, is in this case the nuclear Schiff moment, see Engel (2025) for a recent review. Additional contributions arise from CP-odd electron-nucleus interactions and, for nuclear spin  $\geq 1$ , from higher CP-odd nuclear moments such as the magnetic quadrupole moments (Flambaum (1994)). While the latter can actually dominate certain systems, the main attention in the field has been on the Schiff moment contributions to the atomic EDM.

We can express the Schiff moment of a nucleus  $A$  through a combination of three nuclear quantities

$$S_A = \frac{d_A}{6} (\langle r^2 \rangle_{\text{EDM}} - \langle r^2 \rangle_{\text{charge}}), \quad (57)$$

in terms of the electric dipole radius  $\langle r^2 \rangle_{\text{EDM}}$ , the charge radius  $\langle r^2 \rangle_{\text{charge}}$ , and the nuclear EDM  $d_A$ . The electric dipole radius is defined as the slope of the electric dipole form factor, see Eq. (40), at  $Q^2 = 0$

$$\langle r^2 \rangle_{\text{EDM}} = \frac{6}{d_A} \left. \frac{dF_{\text{EDM}}(Q^2)}{dQ^2} \right|_{Q^2=0}, \quad (58)$$

in analogy to the charge radius. Eq. (57) shows that the Schiff moment vanishes if the electric dipole radius equals the charge radius.

Although experimentally not interesting it can be illuminating to take the hydrogen atom as a case study. While hydrogen is not diamagnetic, having a single unpaired electron, it is still useful to see how the Schiff moment affects the atomic EDM. Since the proton charge radius scales as  $\langle r^2 \rangle_{\text{charge}} \sim 1/\Lambda_\chi^2$  (Bernard et al. (1995)) while the electric dipole radius scales as  $d_p/m_\pi^2$  (see Eqs. (35) and (41)) we observe that for the proton<sup>1</sup>  $S_p \sim d_p/m_\pi^2$ . The Schiff moment leads to a CP-odd atomic Hamiltonian of the form  $H_S \sim eS_A \vec{\sigma} \cdot \vec{\nabla} \delta^3(\vec{r})$  arising from a photon exchange between the atomic electron and the proton Schiff moment. The contact nature can be readily understood in momentum space as the Schiff moment involves two derivatives and the resulting  $\vec{q}^2$  cancels the photon propagator resulting in a contact interaction (Thomas (1995)). The atomic EDM can then be computed in perturbation theory

$$d_{1\text{H}} \sim \sum_{n>1} \frac{\langle 0|er|n\rangle \langle n|H_S|0\rangle}{E_0 - E_n}, \quad (59)$$

where  $|0\rangle$  is the hydrogen ground state and  $|n\rangle$  excited opposite parity states. A quick calculation for  $n = 2$ ,  $l = 1$  states gives the scaling

$$d_{1\text{H}} \sim \alpha_{\text{em}}^2 m_e^2 S_A \sim \alpha_{\text{em}}^2 \frac{m_e^2}{m_\pi^2} d_p, \quad (60)$$

such that the hydrogen EDM is smaller than the proton EDM by a factor  $\alpha_{\text{em}}^2 m_e^2/m_\pi^2 \sim 10^{-9}$ . Schiff screening is very severe. For the deuteron, the  $\chi$ EFT calculations with perturbative pions of the charge radius (Kaplan et al. (1999)) and electric dipole form factor (de Vries et al. (2011b)) show that  $S_d \sim d_D/\gamma^2$  where  $\gamma \simeq m_\pi/3$  is the deuteron binding momentum. The deuterium-to-deuteron EDM is therefore somewhat enhanced over the hydrogen-to-proton EDM.

The arguments above show that atomic EDMs are roughly suppressed by the square of the size of the nucleus over the size of the atom. Naively already for hydrogen-like atoms,  $\alpha_{\text{em}} \rightarrow Z\alpha_{\text{em}}$ , and the amount of screening drops with  $Z^2$ . In addition, electrons become relativistic for larger  $Z$  leading to an increased electron probability density at the nucleus, further reducing the screening to roughly the

<sup>1</sup>This is true for CP-odd sources that break chiral symmetry such as the  $\bar{\theta}$  term. For the qEDM and Weinberg operator the electric dipole radius scales as  $d_p/\Lambda_\chi^2$ .

$10^{-3,-4}$  level explaining why experimental searches target high- $Z$  atoms. Much more detailed calculations can be found in (Dzuba et al. (2002); Ginges and Flambaum (2004)). We write

$$d_A = \kappa_A S_A, \quad (61)$$

and give coefficients for several systems

$$\kappa_{^{129}\text{Xe}} = 3.8 \cdot 10^{-5} \text{ fm}^{-2}, \quad \kappa_{^{199}\text{Hg}} = -2.8 \cdot 10^{-4} \text{ fm}^{-2}, \quad \kappa_{^{225}\text{Ra}} = -7.7 \cdot 10^{-4} \text{ fm}^{-2}, \quad (62)$$

confirming that Schiff screening diminishes for larger systems a bit faster than  $Z^2$ .

The crucial task is then to compute the nuclear Schiff moment  $S_A$  in terms of the CP-odd hadronic interactions in Eq. (34). While light nuclear EDMs have been computed in terms of CP-odd pion-exchange, the three-body force, and short-range interactions, Schiff moments have focused on the pion-exchange pieces. A rough estimate (for nuclei that are not octupole deformed) in terms of  $\bar{g}_{0,1}$  can be obtained by taking a nuclear-mean field approximation and treating the CP-odd pion-exchange as a short-range contact potential. This leads to an estimate (Flambaum et al. (1984); Engel (2025))

$$S_A \simeq 0.06 A^{2/3} \left( \frac{N-Z}{A} \bar{g}_0 - \bar{g}_1 \right) e \text{ fm}^3. \quad (63)$$

For heavy nuclei, the prefactor  $0.06 A^{2/3} = O(1)$ , while  $(N-Z)/A \simeq 1/5$ . For example, for  $^{199}\text{Hg}$  we obtain

$$d_{^{199}\text{Hg}} \simeq \kappa_{^{199}\text{Hg}} (-2\bar{g}_1 + 0.4\bar{g}_0) e \text{ fm}^3 \simeq 5 \cdot 10^{-4} (\bar{g}_1 - 0.2\bar{g}_0) e \text{ fm}, \quad (64)$$

and thus the  $\bar{g}_1$  coefficient is smaller by three orders of magnitude than that of the unscreened deuteron. The simple estimate in Eq. (63) is probably an overestimate as it misses the effects beyond valence nucleons. The so-called ‘core polarization’ (Flambaum et al. (1986); Dmitriev et al. (2005)) gives rise to additional contributions to the Schiff moment. Explicit calculations in various nuclear methods show that they tend to reduce the coefficients, in particular for  $\bar{g}_1$ , sometimes even changing the sign. These cancellations lead to a significantly larger theoretical uncertainty than those affecting EDMs of light nuclei. A compilation of results (Flambaum et al. (1984); Dmitriev et al. (2005); Ban et al. (2010); Yanase and Shimizu (2020)) taken from the review (Engel (2025)) gives

$$d_{^{199}\text{Hg}} \simeq \kappa_{^{199}\text{Hg}} [(0.6 \pm 0.6)\bar{g}_0 + (0.4 \pm 0.8)\bar{g}_1] e \text{ fm}^3, \quad (65)$$

where the uncertainty is arising from the spread in various calculations. The fact that the range includes very small or opposite sign coefficients is worrisome. Furthermore, taking the spread of calculations is hardly a proper estimate of the theoretical uncertainty.

The Schiff moment is also affected by the other LECs in Eq. (34). While the short-range forces have not been systematically studied there are contributions from the nucleon EDMs (Dmitriev and Sen’kov (2003)) and the semi-leptonic tensor operator  $C_T$  (Latha et al. (2009)), modifying the EDM expression into

$$d_{^{199}\text{Hg}} \simeq \kappa_{^{199}\text{Hg}} \left\{ [(1.9 \pm 0.1)d_n + (0.20 \pm 0.06)d_p] \text{ fm}^{-1} + (0.6 \pm 0.6)\bar{g}_0 + (0.4 \pm 0.8)\bar{g}_1 \right\} e \text{ fm}^3 + (1.2 \pm 0.2)(C_T^{(0)} - C_T^{(1)}) \cdot 10^{-7} e \text{ fm}. \quad (66)$$

The indirect limit on the proton EDM is obtained by assuming the other contributions to vanish giving  $d_p \lesssim 10^{-25}$  e cm. However, it is difficult to envision a BSM scenario where  $d_p$  is actually the dominant contribution considering the larger neutron EDM coefficient. In addition, the relative contributions from the nucleon EDMs and CP-odd pion exchange is similar to that of light nuclei, and we can again expect that for sources such as the qCEDM and the FQLR, the  $\bar{g}_{0,1}$  contributions are dominating.

The simple estimate in Eq. (63) does not work for octupole deformed nuclei. In particular,  $^{225}\text{Ra}$  has a close-lying excited nuclear state with a splitting of order tens of keV instead of the typical MeV nuclear splittings (Spevak and Auerbach (1995); Auerbach et al. (1996)). Dobaczewski et al. (2018) showed that there is a correlation between the  $^{225}\text{Ra}$  Schiff moment and the  $^{224,226}\text{Ra}$  octupole moments. The latter are measured guiding the Schiff moments calculations leading to

$$d_{^{225}\text{Ra}} \simeq \kappa_{^{225}\text{Ra}} [(2.5 \pm 7.5)\bar{g}_0 - (64 \pm 37)\bar{g}_1] e \text{ fm}^3, \quad (67)$$

showing much larger coefficients. Despite this enhancement atomic  $^{225}\text{Ra}$  EDM experiments (Bishof et al. (2016)) are not sufficiently precise to compete with  $^{199}\text{Hg}$ , but experiments with molecules containing octupole deformed nuclei such as RaF are very promising (Jadbabaie et al. (2026)). Recently the first beyond-mean-field calculation (Zhou et al. (2025)) of the  $^{225}\text{Ra}$  (and other isotopes) Schiff moment was performed finding somewhat smaller coefficients than Eq. (67). The calculation also uncovered a correlation between the Schiff moment contributions of nuclear intermediate states and their electric dipole transition strengths to the ground state. This connection allows experimental measurements of these transitions to constrain the nuclear models used to calculate the Schiff moments.

In the future it might become possible to perform first-principle nuclear Schiff moment calculations using  $\chi$ EFT in similar spirit as the light-nuclear EDM calculations. Recently, the Schiff moment of  $^{19}\text{F}$  was computed with  $\chi$ EFT wave functions using the no-core shell model (Ng et al. (2026))

$$S_{^{19}\text{F}} = [-(0.38 \pm 0.19)\bar{g}_0 - (0.31 \pm 0.16)\bar{g}_1] e \text{ fm}^3, \quad (68)$$

with 50% uncertainties on the coefficients. The  $S_{^{19}\text{F}}$  can be constrained using the polar molecular measurements on TIF, YbF, and HfF<sup>+</sup>, but, because, the electron density peaks at the heavy nucleus contained in the molecule, the resulting limits are not yet competitive. Nevertheless, the results show the power of ab initio computations and pave the way towards calculations on larger systems. One such calculation was recently performed (Belley et al. (2026)) using the in-medium similarity renormalization group (Hergert et al. (2016)) where Schiff moments

of several light-to-medium heavy nuclei were computed in addition to a calculation of

$$S_{129\text{Xe}} = [-0.27 \bar{g}_0 - 0.13 \bar{g}_1] e \text{ fm}^3. \quad (69)$$

The current limit is  $d_{129\text{Xe}} < 1.5 \cdot 10^{-27} e \text{ cm}$  (Allmendinger et al. (2019)) and thus the sensitivity is not competitive yet with the  $^{199}\text{Hg}$  limits. The xenon calculations are based on a single nuclear interaction and no theoretical uncertainty was given. Cross-checks with other interactions or methods are needed.

The development of first-principle nuclear calculations of symmetry-breaking moments is a very promising direction, but significant work remains. Calculations have focused solely on the CP-odd one-pion-exchange contributions, but already in light nuclei the two-pion-exchange diagrams (Maekawa et al. (2011)) are sizable (Gnech and Viviani (2020)). The effects from the CP-odd three-pion vertex  $\bar{\Delta}$  have not been included in any Schiff moment calculation and the role of CP-odd short-range forces is not systematically investigated. In particular in light of the renormalization issues discussed in Sect. 4.4 the last issue is very pressing. Another open issue is the systematic calculation of nuclear magnetic quadrupole moments (MQM). The  $\chi\text{EFT}$  calculation of the deuteron MQM (Liu et al. (2012)) shows that additional CP-odd hadronic interactions can play a role. Since in several system the nuclear MQM is expected to dominate atomic EDMs (Flambaum (1994); Flambaum et al. (2014)), ab initio calculations of MQMs would be very interesting.

## 6 Paramagnetic electric dipole moments

In paramagnetic systems there is an unpaired electron leading to net electron spin. While Schiff's theorem argues that the electron EDM contribution to the entire neutral system is screened, this can be avoided if relativity is taken into account (Sandars (1965, 1966)). In large atoms or molecules, even valence electrons are relativistic and Schiff's screening can be completely avoided or even overturned: the EDM of a large atom can be larger than that of the electron. Explicit calculations of the enhancement factors are discussed in Ginges and Flambaum (2004). In heavy systems the largest effect arises from the electron EDM interacting with the nuclear charge, leading to a small admixture of opposite parity electron states. Explicit calculations show that this effect leads to a ratio of atomic-to-electron EDM

$$\frac{d_A}{d_e} \equiv K \sim \alpha^2 Z^3 f(Z\alpha), \quad (70)$$

where  $f$  is a monotonically increasing function. As such, the enhancement factor grows 'faster than  $Z^3$ '. For example, for  $^{133}\text{Cs}$  explicit calculations give  $K(\text{Cs}) = 114$  (Hartley et al. (1990)) and for  $^{205}\text{Tl}$   $K(\text{Tl}) = -573$  (Porsev et al. (2012)). Similarly, contributions from the CP-violating scalar nucleon-electron coupling,  $C_S$ , in Eq. (26) are enhanced and are tightly constrained by paramagnetic EDM limits.

Atomic EDMs experiments historically set the strongest electron EDM limits but have now been superseded by molecular measurements. In typical experimental electric fields, atoms are only very weakly polarized because the applied electric field is tiny compared to the internal atomic field that binds the valence electron. In a polar molecule however, there is a near-degenerate opposite parity state with an energy splitting small enough that even the weak laboratory field is sufficient to fully mix them and to completely orient the internuclear axis. This leads to an extra enhancement of  $M_{\text{mol}}/m_e$  (Sushkov and Flambaum (1978)), an astonishing factor of  $O(5 \cdot 10^5)$  for a heavy molecule like ThO, where the molecular mass enters because the doublet splitting is set by the rotational energy scale. Experiments on polar molecules such as YbF (Hudson et al. (2011)), ThO (Andreev et al. (2018)), and HfF<sup>+</sup> (Roussy et al. (2023)) have increased rapidly in the last 15 years and are now by far the best probe of (semi-)leptonic CP violation.

For atoms the induced precession frequency of the atomic spin is linearly dependent on the applied external electric field. For polar molecules, the valence electron feels the internal electric field which is a molecule-dependent quantity that saturates at weak fields and is largely independent of the external field once the molecule is fully polarized. As such, experiments do not report a limit on molecular EDMs but on the observed frequency shift. This frequency shift can be expressed in contributions from the electron EDM,  $d_e$ , and CP-violating electron-nucleon interactions. For example

$$\omega_{\text{HF}} = (34.9 \pm 1.4)(\text{mrad/s}) \left( \frac{d_e}{10^{-27} e \text{ cm}} \right) + (32.0 \pm 1.3)(\text{mrad/s}) \left( \frac{C_S}{10^{-7}} \right), \quad (71)$$

where the coefficients in front of  $d_e$  and  $C_S$  are molecular matrix elements obtained with relativistic many-body calculations (Skripnikov (2017); Fleig and Jung (2018); Haase et al. (2021)). Assuming  $C_S = 0$  and using the limit on  $\omega_{\text{HF}}$  (Roussy et al. (2023)) then leads to  $d_e < 4.1 \cdot 10^{-30} e \text{ cm}$ . Since limits on EDMs are easier to interpret than limits on frequencies, Pospelov and Ritz (2014) suggested to interpret paramagnetic EDM measurements in terms of the 'equivalent' electron EDM defined as

$$d_e^{\text{equiv}} = d_e + r_A C_S, \quad (72)$$

where  $r_A$  is a molecule dependent ratio of molecular matrix elements, for example,

$$r_{\text{BaF}} = 4.5 \cdot 10^{-21} e \text{ cm}, \quad r_{\text{ThO}} = 1.5 \cdot 10^{-20} e \text{ cm}, \quad r_{\text{HfF}^+} = 9.2 \cdot 10^{-21} e \text{ cm}. \quad (73)$$

The fact that these ratios are not precisely the same implies that measurements on several systems can unravel the electron EDM from  $C_S$ .

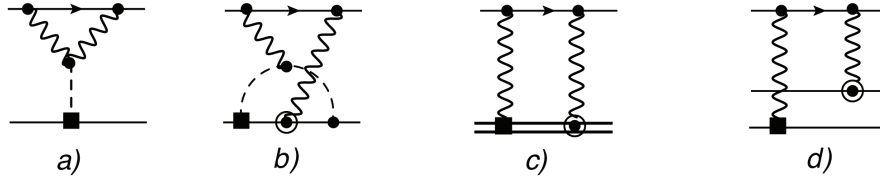


Fig. 4: Several diagrams contributing to a CP-violating electron-nuclear interaction. The top solid arrowed line is the electron and the other solid lines are nucleons. The double line in diagram c) denotes the nucleus as a whole. Wavy and dashed lines are photons and pions. The black square is a CP-odd interaction while black circles denote CP-even interactions. The circled circle in diagram b), c), d) denotes the nucleon or nuclear magnetic moment.

### 6.1 Using paramagnetic EDMs to probe hadronic CP violation

The discussion so far has mainly focused on the electron EDM and the CP-odd electron-nucleon coupling  $C_S$  as the quantities directly constrained by paramagnetic EDM experiments. While the electron EDM can be computed directly in the SM or in beyond-the-SM scenarios,  $C_S$  is an effective hadronic interaction that must be expressed in terms of more fundamental source of CP violation. The most obvious source are the four-fermion electron-quark interactions in Eq. (10). In this way, stringent limits on CP violation in, for example, leptoquark models can be derived (Dekens et al. (2019)).

More intricate contributions to  $C_S$  have been the focus of more recent studies. The key observation (Flambaum et al. (2020); Mulder et al. (2025); Dekens et al. (2026)), is that paramagnetic experiments are also sensitive to hadronic CP violation and that this sensitivity is complementary to and competitive with dedicated hadronic EDM searches. The main physical mechanism is the following. As discussed in Sect. 3, sources of hadronic CP violation that violate chiral symmetry, such as the  $\bar{\theta}$  term, qCEDMs, or the FQLR, generate CP-odd pion-nucleon couplings  $\bar{g}_{0,1}$ . The CP-odd pion-nucleon couplings generate a virtual neutral pion in the system which then couples to two photons through the chiral anomaly and the photons, in turn, couple to an electron (see Fig. 4a)). The resulting effective interaction is precisely the scalar-pseudoscalar electron-nucleon coupling  $C_S$  of Eq. (26).

For  $\bar{g}_1$  this effect is coherent over all nucleons in the nucleus and thus picks up an overall factor  $A$  while for  $\bar{g}_0$  a relative  $(Z - N)/A$  suppression appears. This implies that for the  $\bar{\theta}$  term, for which  $\bar{g}_0$  is the only leading-order CP-violating interaction, formally next-to-leading order interactions are relevant. These involve isospin-breaking corrections through  $\bar{g}_1$ , strangeness corrections through  $\eta$  exchange, and two-loop pion-photon loops (Fig. 4b)). Combined (Mulder et al. (2025)) gives the following result for the nucleus-averaged coupling

$$C_S = \frac{\sqrt{2}}{G_F} \frac{\alpha^2}{4\pi^2} \frac{m_e}{F_\pi m_\pi^2} \left\{ \left[ \frac{Z - N}{Z + N} \bar{g}_0 + \bar{g}_1 \right] \mathcal{B}^\pi + \frac{F_\pi}{\sqrt{3} F_\eta} \frac{m_\pi^2}{m_\eta^2} \bar{g}_{0\eta} \mathcal{B}^\eta + \bar{g}_0 \frac{\pi g_A m_\pi}{m_N} \frac{Z\mu_n - N\mu_p}{(Z + N)} \left[ \log \left( \frac{m_\pi}{m_e} \right) + 1.77 \right] \right\}, \quad (74)$$

where  $B^\pi \simeq B^\eta \simeq 45$  are renormalized one-loop diagrams, and  $\mu_n = -1.91$ ,  $\mu_p = 2.79$  are the nucleon magnetic moments in units of the nuclear magneton. The term in brackets proportional to the magnetic moments is the result of a numerical evaluation of a two-loop integral. Plugging in values of the  $\bar{g}_{0,1}$  and  $\bar{g}_{0\eta}$  (taken from de Vries et al. (2015)) for  $\bar{\theta}$  and using typical  $N, Z$  values gives

$$C_S(\bar{\theta}) = (1.63 \pm 0.45) \cdot 10^{-2} \bar{\theta}, \quad (75)$$

or, equivalently, for  $\text{HfF}^+$ ,

$$d_e^{\text{equiv}}(\bar{\theta}) = (1.50 \pm 0.42) \cdot 10^{-22} \bar{\theta} \text{ e cm}, \quad (76)$$

and thus the paramagnetic bound gives  $\bar{\theta} < 1.5 \cdot 10^{-8}$  roughly two orders of magnitude weaker than the traditional limit obtained from the neutron EDM. This bound does not include contributions from nucleon EDMs discussed below. In similar fashion, bounds can be set on other CP-violating hadronic sources. For the qCEDM and FQLR, the  $\bar{g}_1$  contribution is dominant and the other terms in Eq. (74) can be neglected.

Additional contributions to paramagnetic EDMs can arise from a combination of nucleon electric and magnetic dipole moments (Flambaum et al. (2020), Dekens et al. (2026)). These contributions, shown in Figs. 4c) and 4d) are particularly relevant for hadronic sources, such as the qEDM or the Weinberg operator, for which the CP-violating pion-nucleon couplings are suppressed. For diagram 4c) it is no longer valid to talk about CP-odd interactions between electrons and individual nucleons, but rather between electrons and the nucleus as a whole. I denote this coupling by  $\bar{C}_S$ . In the first diagram, the exchanged photons have virtuality of the order of nuclear excitation energies  $\Delta_n$  around a few MeV. Under the assumption that  $\Delta_n \gg m_e$ , the expression for  $\bar{C}_S$  becomes compact

$$\bar{C}_S = -\frac{\sqrt{2}}{G_F} \frac{4\alpha^2 m_e}{m_N} \sum_n \frac{A_n}{\Delta_n} \left( 3 \ln \frac{m_e^2}{4\Delta_n^2} - 1 \right), \quad A_n = -\frac{\langle h_i | D \vec{\sigma} | n \rangle \cdot \langle n | \mu \vec{\sigma} | h_i \rangle}{12}. \quad (77)$$

Here  $A_n$  is a nuclear matrix elements between the ground state  $|h_i\rangle$  and  $1^+$  nuclear excited states  $|n\rangle$  involving the EDM ( $D$ ) and magnetic dipole ( $\mu$ ) operator. The calculation of  $A_n$  is difficult as it requires a sum over many states. An explicit nuclear shell model calculation was performed for BaF (Dekens et al. (2026)) for which a first limit was recently reported (Boeschoten et al. (2026)) leading to

$$\bar{C}_S(\text{BaF}) = (67 \pm 28) \frac{d_p}{\text{e fm}}. \quad (78)$$

Most of the contributions arises from  $1^+$  excited states with energies around 4 to 5 MeV and higher states contribute little. The absence of a neutron EDM contribution is specific to  $^{138}\text{Ba}$  which has a magic neutron number. It would be interesting to perform similar computations for the larger ThO and HfF $^+$  systems.

Diagram 4d) involves two separate nucleons in a nucleus. The resulting value of  $\bar{C}_S$ , the effective CP-odd electron-nucleus coupling, involves the calculations of a ground-state to ground-state two-nucleon matrix element

$$\bar{C}_S = -\frac{\sqrt{2}}{G_F} \langle h_i | V | h_i \rangle, \quad V = \frac{4e^4 m_e}{9m_N} \sum_{i \neq j} \frac{\mu^{(i)} D^{(j)}}{|\vec{q}|^4} \left[ \vec{\sigma}^{(i)} \cdot \vec{\sigma}^{(j)} - \frac{1}{4} S^{(ij)} \right], \quad (79)$$

where  $\vec{q}$  is the momentum transfer and  $S^{(ij)} = \vec{\sigma}^{(i)} \cdot \vec{\sigma}^{(j)} - 3(\vec{q} \cdot \vec{\sigma}^{(i)})(\vec{q} \cdot \vec{\sigma}^{(j)})/|\vec{q}|^2$  is a tensor operator. Explicit nuclear shell model calculations for a range of nuclei show that the effect is coherent and scales with the number of neutrons and protons. For BaF in particular

$$\bar{C}_S(\text{BaF}) = [(-433 \pm 5) d_p + (387 \pm 0.4) d_n] (e \text{ fm})^{-1}, \quad (80)$$

several times larger than Eq. (78). The coherence can be used to compute the result for a general polar molecule containing a heavy nucleus  $A$  with  $Z$  protons and  $N$  neutrons

$$d_e^{\text{equiv}} = \frac{\sqrt{2} e^4 m_e}{18\pi G_F m_N} \frac{r_A}{A} (-9.7) [Z \mu_p d_p + N \mu_n d_n] \frac{\text{fm}}{e}, \quad (81)$$

where the  $-9.7$  is a numerical coefficient computed with the shell model with an expected 25% uncertainty mainly from higher-order chiral corrections. This formula makes it possible to constrain nucleon EDMs from the most precise HfF $^+$  measurement. Because  $Z\mu_p \approx -N\mu_n$  for heavy nuclei, the paramagnetic molecules mainly constrains the isovector combination

$$|d_n - d_p| < 1.6 \cdot 10^{-23} e \text{ cm}. \quad (82)$$

The direct neutron EDM limit is stronger by three orders of magnitude, while the inferred proton EDM limit from the  $^{199}\text{Hg}$  measurement is a hundred times stronger.

The above discussion shows that paramagnetic EDM measurements are becoming 'diamagnetic' in the sense that they can constrain CP-violating sources in the quark-gluon sector through distinct and calculable mechanisms. The interpretation of future measurements in terms of all these contributions simultaneously will require combining results from several molecular systems with different  $r_A$  ratios and will demand continued progress in both nuclear structure calculations and chiral EFT matching. While in absolute limits there is still a gap of two-to-three orders of magnitude in sensitivity, the paramagnetic EDM limits have made much faster progress and a further reduction of the gap is definitely possible. Perhaps more importantly, the experiments are complementary as the ratio of paramagnetic-to-diamagnetic EDMs can be used to identify the underlying CP-violating mechanism. This will be discussed in the next section.

## 7 Unraveling the mechanism of CP violation with the EDM portfolio

While squarely in the category of problems one hopes to face, a measurement of a nonzero EDM immediately raises the question of which source is responsible. Assuming the discovery is made in the foreseeable future, we can rule out the CKM mechanism (Pospelov and Ritz (2014)), leaving either the  $\bar{\theta}$  term or a BSM source of CP violation as the explanation. Identifying the  $\bar{\theta}$  term as the source would have far-reaching consequences for the strong CP problem.

Solutions to the strong CP problem fall into two broad classes (Craig (2023)): UV solutions, where CP or P is an exact symmetry that is spontaneously broken at high energies (Nelson (1984); Barr (1984); Babu and Mohapatra (1990)), and IR solutions such as the Peccei-Quinn mechanism (Peccei and Quinn (1977)), where  $\bar{\theta}$  is relaxed to zero dynamically at low energies. Generically, UV solutions do not predict new sources of hadronic CP violation beyond  $\bar{\theta}$ , because the symmetry protecting  $\bar{\theta}$  also suppresses other CP-odd dimension-six operators below observable levels. To be clear, this is a naturalness argument which, as history shows, have not always been reliable. Nevertheless, from an EFT perspective it is difficult to understand why  $\bar{\theta}$  remains small in the IR if other hadronic CP-violating sources are present. A pattern of EDMs consistent with a BSM hadronic source but inconsistent with a  $\bar{\theta}$ -dominated scenario would therefore point toward an IR solution, such as the Peccei-Quinn mechanism, as the explanation for the smallness of  $\bar{\theta}$  (de Vries et al. (2021a); Choi et al. (2024); Choi and Im (2026)). On the other hand, if the source of CP violation is not the  $\bar{\theta}$  term, identifying which BSM operator is responsible becomes equally important as it would inform us about the possible UV completions, guide complementary searches at colliders and low-energy precision experiments, and shed light on viable mechanisms of electroweak baryogenesis.

If nonzero EDMs are measured, the first question is whether the source is (semi-)leptonic or hadronic. This can be determined through the ratio of paramagnetic EDMs over neutron/diamagnetic EDMs. If the paramagnetic EDMs are relatively large, the source is most likely the electron EDM,  $d_e$  or the CP-odd electron-nucleon interactions  $C_S$ . By comparing the ratio of several paramagnetic systems with different  $r_A$  coefficients, see Eq. (72), it should be possible to determine the origin (Chupp et al. (2019); Fleig and Jung (2018)).

If the source is hadronic, the first question should be whether the pattern of EDMs is consistent with the  $\bar{\theta}$  term. All calculations indicate the nucleon EDMs induced by  $\bar{\theta}$  are mainly isovector and thus  $d_n$  and  $d_p$  appear with opposite sign. In addition, this implies that the deuteron EDM is relatively small because both  $d_n + d_p$  and  $\bar{g}_1$  are small for  $\bar{\theta}$ , while  $^3\text{He}$  can be expected to be larger. This pattern of nucleon and light nuclear EDMs is shown in the left panel of Fig. 5. However experiments probing EDMs of light nuclei are currently not competitive. The limit on the  $^{199}\text{Hg}$  EDM is very strong but the large nuclear uncertainties of the  $\bar{g}_0$  coefficient makes a determination more difficult.

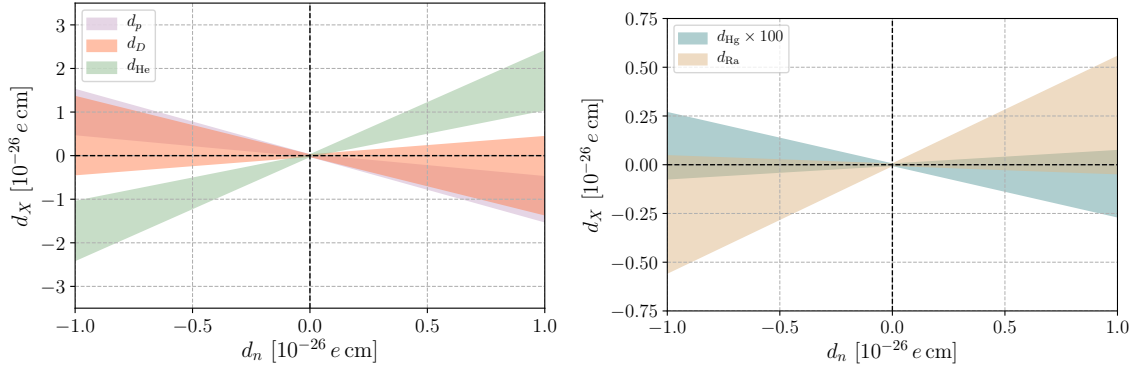


Fig. 5: Left panel: Correlation between various EDMs (proton and light nuclei) and the neutron EDM in case the  $\bar{\theta}$  term is the underlying CP-violating mechanism. The bands indicate the theoretical uncertainty. EDM measurements that would fall outside the shared areas, points towards a BSM CP-violating source and, indirectly, towards an IR solutions of the strong CP problem. Right panel: the same but now for EDMs of diamagnetic EDMs versus the neutron EDM. Here the nuclear uncertainty typically leads to broader uncertainty bands. Figure adapted from de Vries et al. (2019).

The same is true for  $^{225}\text{Ra}$ , see the right panel of Fig. 5. Interestingly, paramagnetic systems, through Eq. (75) and Eq. (81), can also be used to identify the presence of  $\bar{\theta}$  as it predicts, for example, the  $\omega_{\text{HF}}/d_n$  ratio (Dekens et al. (2026)).

If the source is not  $\bar{\theta}$ , there are several options. The qCEDM and FQLR predict that nuclear and diamagnetic EDMs are dominated by the CP-odd nuclear forces mainly through a large  $\bar{g}_1$  coefficient (and possibly  $\bar{\Delta}$  although the role of three-nucleon CP-odd forces is unclear). This means that these sources tend to predict larger  $d_D/d_n$  and  $d_{\text{Ra}}/d_n$  ratios than the  $\bar{\theta}$  term. The qEDM and Weinberg operator predict that nuclear and diamagnetic EDMs are mainly functions of the nucleon EDMs and no large ratios are expected.

The above predictions are subject to substantial hadronic and nuclear uncertainties. For sources beyond  $\bar{\theta}$  and qEDMs, the CP-odd LECs are currently known only at the order-of-magnitude level, and the role of short-range CP-odd nuclear forces, three-body interactions, and subleading pion-exchange corrections remains poorly understood beyond light nuclei. Reducing these uncertainties, through lattice QCD determinations of the hadronic LECs and ab initio nuclear calculations for heavier systems, is essential if a future EDM signal is to be unambiguously traced back to its origin.

## 8 Conclusion

This review has presented the theory of electric dipole moments from a low-energy perspective, tracing the chain of connections that links CP-violating interactions at the quark and gluon level to observable EDMs of nucleons, nuclei, atoms, and molecules. Starting from a general CP-odd effective Lagrangian at the hadronic matching scale, comprising the  $\bar{\theta}$  term, quark EDMs and chromo-EDMs, the Weinberg operator, and CP-odd four-fermion interactions, chiral perturbation theory organizes the nonperturbative QCD dynamics into a small set of hadronic LECs. The nuclear EDMs and Schiff moments of light and heavy nuclei were then discussed within chiral EFT, emphasizing the power counting that identifies the leading CP-odd pion-exchange mechanisms and the role of short-range CP-odd forces whose status is still unclear. At the atomic and molecular level, we covered both diamagnetic systems, where sensitivity to hadronic CP violation is mediated by nuclear Schiff moments and related CP-odd moments, and paramagnetic systems, where the dominant sensitivity is to the electron EDM and the scalar electron-nucleon coupling  $C_S$ . We discussed how hadronic CP violation can enter paramagnetic systems through a recently identified and still largely unexplored set of mechanisms. The complementarity of the full EDM portfolio, encompassing nucleons, light nuclei, diamagnetic atoms, and polar molecules, in disentangling the underlying source of CP violation was discussed in the final section.

While not covered in this review, the experimental prospects for EDM searches are excellent. Sensitivity to paramagnetic EDMs has already improved by more than two orders of magnitude in the past 15 years. Looking ahead, technological advances across all categories of EDM experiments, from improved neutron EDM measurements, to novel molecular cooling and trapping techniques, to using radioactive species, to storage ring experiments, promise to further push the sensitivity in upcoming years.

The theory of EDMs faces challenges and opportunities at every layer of the hierarchy. At the hadronic level, the determination of the CP-odd LECs for sources beyond the  $\bar{\theta}$  term remains a pressing open problem. The gradient-flow approach to lattice QCD, for which the perturbative one-loop matching of all relevant operators has recently been completed, offers a realistic path toward first-principles determinations of these LECs. At the nuclear level, the extension of ab initio many-body methods to heavier octupole-deformed nuclei such as  $^{225}\text{Ra}$ , and the systematic inclusion of the complete set of CP-odd forces, including short-range and three-body interactions, in nuclear calculations of Schiff and magnetic quadrupole moments, is essential to exploit the current and next generation of diamagnetic experiments. At the molecular level, the connection between hadronic CP violation and paramagnetic observables is only beginning to be mapped out. The view from below, from the mud of hadronic, nuclear, and molecular physics, will become increasingly important as experimental sensitivity improves: a future EDM signal will only reveal the underlying mechanism of CP violation if the theoretical chain

from elementary particles to observables is quantitatively under control at every step.

## Acknowledgements

I thank Heleen Mulder and Lemonia Gialidi for comments on the manuscript and help with the figures. I am grateful to Emanuele Mereghetti, Wouter Dekens, and Vincenzo Cirigliano for discussions on some of the topics presented here. I thank Bira van Kolck and Rob Timmermans for introducing me to this field all those years ago, and the EDM community at large for providing a rich and collegial research environment. JdV is supported by the ERC COG grant CRUNS, 101230525, and by Dutch Research Council (NWO) in the form of a VIDI grant.

## References

- Abe T, Hisano J and Nagai R (2018). Model independent evaluation of the Wilson coefficient of the Weinberg operator in QCD. *JHEP* 03: 175. doi:10.1007/JHEP03(2018)175. [Erratum: *JHEP* 09, 020 (2018)], 1712.09503.
- Abel C and et al. (2020). Measurement of the Permanent Electric Dipole Moment of the Neutron. *Phys. Rev. Lett.* 124 (8): 081803. doi:10.1103/PhysRevLett.124.081803. 2001.11966.
- Adelmann A and et al. (2025). A compact frozen-spin trap for the search for the electric dipole moment of the muon. *Eur. Phys. J. C* 85 (6): 622. doi:10.1140/epjc/s10052-025-14295-7. 2501.18979.
- Afnan IR and Gibson BF (2010). Model Dependence of the 2H Electric Dipole Moment. *Phys. Rev. C* 82: 064002. doi:10.1103/PhysRevC.82.064002. 1011.4968.
- Alarcon R and et al. (2022), 3, Electric dipole moments and the search for new physics, Snowmass 2021, 2203.08103.
- Alexander J and et al. (pEDM) (2022), 4. The storage ring proton EDM experiment 2205.00830.
- Allmendinger F, Engin I, Heil W, Karpuk S, Krause HJ, Niederländer B, Offenhäusser A, Repetto M, Schmidt U and Zimmer S (2019), Aug. Measurement of the permanent electric dipole moment of the  $^{129}\text{Xe}$  atom. *Phys. Rev. A* 100: 022505. doi:10.1103/PhysRevA.100.022505. <https://link.aps.org/doi/10.1103/PhysRevA.100.022505>.
- Andreev V and et al. (ACME) (2018). Improved limit on the electric dipole moment of the electron. *Nature* 562 (7727): 355–360. doi:10.1038/s41586-018-0599-8.
- Andres A and et al. (2026), 2. First Experimental Limit on the Permanent Electric Dipole Moment of the Deuteron 2602.20828.
- Aoki Y and et al. (Flavour Lattice Averaging Group (FLAG)) (2026). FLAG review 2024. *Phys. Rev. D* 113 (1): 014508. doi:10.1103/nfzp-p5dn.2411.04268.
- Auerbach N, Flambaum VV and Spevak V (1996). Collective T and P odd electromagnetic moments in nuclei with octupole deformations. *Phys. Rev. Lett.* 76: 4316–4319. doi:10.1103/PhysRevLett.76.4316. nucl-th/9601046.
- Babu KS and Mohapatra RN (1990). A Solution to the Strong CP Problem Without an Axion. *Phys. Rev. D* 41: 1286. doi:10.1103/PhysRevD.41.1286.
- Baluni V (1979). CP Violating Effects in QCD. *Phys. Rev. D* 19: 2227–2230. doi:10.1103/PhysRevD.19.2227.
- Ban S, Dobaczewski J, Engel J and Shukla A (2010). Fully self-consistent calculations of nuclear Schiff moments. *Phys. Rev. C* 82: 015501. doi:10.1103/PhysRevC.82.015501. 1003.2598.
- Barr SM (1984). Solving the Strong CP Problem Without the Peccei-Quinn Symmetry. *Phys. Rev. Lett.* 53: 329. doi:10.1103/PhysRevLett.53.329.
- Barr SM and Zee A (1990). Electric Dipole Moment of the Electron and of the Neutron. *Phys. Rev. Lett.* 65: 21–24. doi:10.1103/PhysRevLett.65.21. [Erratum: *Phys. Rev. Lett.* 65, 2920 (1990)].
- Bartolini L, Bigazzi F, Bolognesi S, Cotrone AL and Manenti A (2017). Neutron electric dipole moment from gauge/string duality. *Phys. Rev. Lett.* 118 (9): 091601. doi:10.1103/PhysRevLett.118.091601. 1609.09513.
- Bartolini L, Bolognesi S and Gudnason SB (2020). Deuteron electric dipole moment from holographic QCD. *Phys. Rev. D* 101 (8): 086009. doi:10.1103/PhysRevD.101.086009. 1912.01641.
- Belley A and et al. (2026), 5. Ab initio calculation of symmetry-breaking observables 2605.11353.
- Bernard V, Kaiser N and Meissner UG (1995). Chiral dynamics in nucleons and nuclei. *Int. J. Mod. Phys. E* 4: 193–346. doi:10.1142/S0218301395000092. hep-ph/9501384.
- Bhattacharya T, Bhattacharya S, Cirigliano V, Gupta R, Mereghetti E, Park S, Yoo JS and Yoon B (2025). Gradient Flow of the Weinberg Operator. *PoS LATTICE2024*: 344. doi:10.22323/1.466.0344. 2502.00460.
- Bischof M and et al. (2016). Improved limit on the  $^{225}\text{Ra}$  electric dipole moment. *Phys. Rev. C* 94 (2): 025501. doi:10.1103/PhysRevC.94.025501. 1606.04931.
- Boeschoten A and et al. (2026). Statistics and systematics of electron EDM searches with BaF. *Eur. Phys. J. D* 80 (5): 62. doi:10.1140/epjd/s10053-026-01175-2. 2601.21781.
- Borasoy B (2000). The Electric dipole moment of the neutron in chiral perturbation theory. *Phys. Rev. D* 61: 114017. doi:10.1103/PhysRevD.61.114017. hep-ph/0004011.
- Braaten E, Li CS and Yuan TC (1990). The Gluon Color - Electric Dipole Moment and Its Anomalous Dimension. *Phys. Rev. D* 42: 276–278. doi:10.1103/PhysRevD.42.276.
- Brod J, Polonsky Z and Stamou E (2024). A precise electron EDM constraint on CP-odd heavy-quark Yukawas. *JHEP* 06: 091. doi:10.1007/JHEP06(2024)091. 2306.12478.
- Bsaisou J, Hanhart C, Liebig S, Meissner UG, Nogga A and Wirzba A (2013). The electric dipole moment of the deuteron from the QCD  $\theta$ -term. *Eur. Phys. J. A* 49: 31. doi:10.1140/epja/i2013-13031-x. 1209.6306.
- Bsaisou J, de Vries J, Hanhart C, Liebig S, Meissner UG, Minossi D, Nogga A and Wirzba A (2015a). Nuclear Electric Dipole Moments in Chiral Effective Field Theory. *JHEP* 03: 104. doi:10.1007/JHEP03(2015)104. [Erratum: *JHEP* 05, 083 (2015)], 1411.5804.
- Bsaisou J, Meißner UG, Nogga A and Wirzba A (2015b). P- and T-Violating Lagrangians in Chiral Effective Field Theory and Nuclear Electric Dipole Moments. *Annals Phys.* 359: 317–370. doi:10.1016/j.aop.2015.04.031. 1412.5471.
- Buchmüller W and Wyler D (1983). CP Violation and R Invariance in Supersymmetric Models of Strong and Electroweak Interactions. *Phys. Lett. B* 121: 321. doi:10.1016/0370-2693(83)91378-3.

- Buchmuller W and Wyler D (1986). Effective Lagrangian Analysis of New Interactions and Flavor Conservation. *Nucl. Phys. B* 268: 621–653. doi:10.1016/0550-3213(86)90262-2.
- Bühler J and Stoffer P (2023). One-loop matching of CP-odd four-quark operators to the gradient-flow scheme. *JHEP* 08: 194. doi:10.1007/JHEP08(2023)194. 2304.00985.
- Choi K and Im SH (2026), 4. The EDM inverse problem: Identifying the sources of CP violation and PQ breaking with electric dipole moments 2604.25516.
- Choi K, Im SH and Jodłowski K (2024). Exploring CP violation beyond the Standard Model and the PQ quality with electric dipole moments. *JHEP* 04: 007. doi:10.1007/JHEP04(2024)007. 2308.01090.
- Chupp T, Fierlinger P, Ramsey-Musolf M and Singh J (2019). Electric dipole moments of atoms, molecules, nuclei, and particles. *Rev. Mod. Phys.* 91 (1): 015001. doi:10.1103/RevModPhys.91.015001. 1710.02504.
- Cirigliano V, Dekens W, De Vries J, Graesser ML, Mereghetti E, Pastore S and Van Kolck U (2018). New Leading Contribution to Neutrinoless Double- $\beta$  Decay. *Phys. Rev. Lett.* 120 (20): 202001. doi:10.1103/PhysRevLett.120.202001. 1802.10097.
- Cirigliano V, Mereghetti E and Stoffer P (2020). Non-perturbative renormalization scheme for the  $CP$ -odd three-gluon operator. *JHEP* 09: 094. doi:10.1007/JHEP09(2020)094. 2004.03576.
- Cottingham WN (1963). The neutron proton mass difference and electron scattering experiments. *Annals Phys.* 25: 424–432. doi:10.1016/0003-4916(63)90023-X.
- Craig N (2023). Naturalness: past, present, and future. *Eur. Phys. J. C* 83 (9): 825. doi:10.1140/epjc/s10052-023-11928-7. 2205.05708.
- Crewther RJ, Di Vecchia P, Veneziano G and Witten E (1979). Chiral Estimate of the Electric Dipole Moment of the Neutron in Quantum Chromodynamics. *Phys. Lett. B* 88: 123. doi:10.1016/0370-2693(79)90128-X. [Erratum: *Phys.Lett.B* 91, 487 (1980)].
- de Vries J, Higa R, Liu CP, Mereghetti E, Stetcu I, Timmermans RGE and van Kolck U (2011a). Electric Dipole Moments of Light Nuclei From Chiral Effective Field Theory. *Phys. Rev. C* 84: 065501. doi:10.1103/PhysRevC.84.065501. 1109.3604.
- de Vries J, Mereghetti E, Timmermans RGE and van Kolck U (2011b). Parity- and Time-Reversal-Violating Form Factors of the Deuteron. *Phys. Rev. Lett.* 107: 091804. doi:10.1103/PhysRevLett.107.091804. 1102.4068.
- de Vries J, Timmermans RGE, Mereghetti E and van Kolck U (2011c). The Nucleon Electric Dipole Form Factor From Dimension-Six Time-Reversal Violation. *Phys. Lett. B* 695: 268–274. doi:10.1016/j.physletb.2010.11.042. 1006.2304.
- de Vries J, Mereghetti E, Timmermans RGE and van Kolck U (2013). The Effective Chiral Lagrangian From Dimension-Six Parity and Time-Reversal Violation. *Annals Phys.* 338: 50–96. doi:10.1016/j.aop.2013.05.022. 1212.0990.
- de Vries J, Mereghetti E and Walker-Loud A (2015). Baryon mass splittings and strong CP violation in SU(3) Chiral Perturbation Theory. *Phys. Rev. C* 92 (4): 045201. doi:10.1103/PhysRevC.92.045201. 1506.06247.
- de Vries J, Draper P, Fuyuto K, Kozaczuk J and Sutherland D (2019). Indirect Signs of the Peccei-Quinn Mechanism. *Phys. Rev. D* 99 (1): 015042. doi:10.1103/PhysRevD.99.015042. 1809.10143.
- de Vries J, Epelbaum E, Girlanda L, Gnech A, Mereghetti E and Viviani M (2020a). Parity- and Time-Reversal-Violating Nuclear Forces. *Front. in Phys.* 8: 218. doi:10.3389/fphy.2020.00218. 2001.09050.
- de Vries J, Falcioni G, Herzog F and Ruij B (2020b). Two- and three-loop anomalous dimensions of Weinberg's dimension-six CP-odd gluonic operator. *Phys. Rev. D* 102 (1): 016010. doi:10.1103/PhysRevD.102.016010. 1907.04923.
- de Vries J, Draper P, Fuyuto K, Kozaczuk J and Lillard B (2021a). Uncovering an axion mechanism with the EDM portfolio. *Phys. Rev. D* 104 (5): 055039. doi:10.1103/PhysRevD.104.055039. 2107.04046.
- de Vries J, Gnech A and Shain S (2021b). Renormalization of  $CP$ -violating nuclear forces. *Phys. Rev. C* 103 (1): L012501. doi:10.1103/PhysRevC.103.L012501. 2007.04927.
- Degenkolb S, Elmer N, Modak T, Mühlleitner M and Plehn T (2026). A Global View of the EDM Landscape. *SciPost Phys.* 20: 151. doi:10.21468/SciPostPhys.20.6.151. 2403.02052.
- Degrassi G, Franco E, Marchetti S and Silvestrini L (2005). QCD corrections to the electric dipole moment of the neutron in the MSSM. *JHEP* 11: 044. doi:10.1088/1126-6708/2005/11/044. hep-ph/0510137.
- Dekens W and de Vries J (2013). Renormalization Group Running of Dimension-Six Sources of Parity and Time-Reversal Violation. *JHEP* 05: 149. doi:10.1007/JHEP05(2013)149. 1303.3156.
- Dekens W, de Vries J, Bsaisou J, Bernreuther W, Hanhart C, Meißner UG, Nogga A and Wirzba A (2014). Unraveling models of CP violation through electric dipole moments of light nuclei. *JHEP* 07: 069. doi:10.1007/JHEP07(2014)069. 1404.6082.
- Dekens W, de Vries J, Jung M and Vos KK (2019). The phenomenology of electric dipole moments in models of scalar leptoquarks. *JHEP* 01: 069. doi:10.1007/JHEP01(2019)069. 1809.09114.
- Dekens W, de Vries J and Shain S (2022). CP-violating axion interactions in effective field theory. *JHEP* 07: 014. doi:10.1007/JHEP07(2022)014. 2203.11230.
- Dekens W, de Vries J, Gialidi L, Menéndez J, Mulder H and Romeo B (2026). Nucleon Electric Dipole Moments in Paramagnetic Molecules through Effective Field Theory. *Phys. Rev. Lett.* 136 (20): 201803. doi:10.1103/5rpp-f6h4. 2510.14933.
- Demir DA, Pospelov M and Ritz A (2003). Hadronic EDMs, the Weinberg operator, and light gluinos. *Phys. Rev. D* 67: 015007. doi:10.1103/PhysRevD.67.015007. hep-ph/0208257.
- Dib C, Faessler A, Gutsche T, Kovalenko S, Kuckei J, Lyubovitskij VE and Pumsa-ard K (2006). The Neutron electric dipole form-factor in the perturbative chiral quark model. *J. Phys. G* 32: 547–564. doi:10.1088/0954-3899/32/4/011. hep-ph/0601144.
- Dmitriev VF and Sen'kov RA (2003). Schiff moment of the mercury nucleus and the proton dipole moment. *Phys. Rev. Lett.* 91: 212303. doi:10.1103/PhysRevLett.91.212303. nucl-th/0306050.
- Dmitriev VF, Sen'kov RA and Auerbach N (2005). Effects of core polarization on the nuclear Schiff moment. *Phys. Rev. C* 71: 035501. doi:10.1103/PhysRevC.71.035501. nucl-th/0408065.
- Dobaczewski J, Engel J, Kortelainen M and Becker P (2018). Correlating Schiff moments in the light actinides with octupole moments. *Phys. Rev. Lett.* 121 (23): 232501. doi:10.1103/PhysRevLett.121.232501. 1807.09581.
- Dragos J, Luu T, Shindler A, de Vries J and Yousif A (2021). Confirming the Existence of the strong CP Problem in Lattice QCD with the Gradient Flow. *Phys. Rev. C* 103 (1): 015202. doi:10.1103/PhysRevC.103.015202. 1902.03254.
- Dutsov C, Hume T, Pospelov M and Schmidt-Wellenburg P (2025). Experimental search for electric dipole moments of light radioactive nuclei. *Phys. Rev. D* 112 (7): 076031. doi:10.1103/hi5s-dqqw. 2506.13588.
- Dzuba VA, Flambaum VV, Ginges JSM and Kozlov MG (2002). Electric dipole moments of Hg, Xe, Rn, Ra, Pu, and Tl induced by the nuclear Schiff moment and limits on time reversal violating interactions. *Phys. Rev. A* 66: 012111. doi:10.1103/PhysRevA.66.012111. hep-ph/0203202.
- Ellis JR, Ferrara S and Nanopoulos DV (1982). CP Violation and Supersymmetry. *Phys. Lett. B* 114: 231–234. doi:10.1016/0370-2693(82)90484-1.
- Ema Y, Gao T and Pospelov M (2022). Standard Model Prediction for Paramagnetic Electric Dipole Moments. *Phys. Rev. Lett.* 129 (23): 231801. doi:10.1103/PhysRevLett.129.231801. 2202.10524.
- Engel J (2025). Nuclear Schiff Moments and CP Violation. *Ann. Rev. Nucl. Part. Sci.* 75 (1): 129–151. doi:10.1146/annurev-nucl-121423-101030.

- 2501.02744.
- Engel J, Friar JL and Hayes AC (2000). Nuclear octupole correlations and the enhancement of atomic time reversal violation. *Phys. Rev. C* 61: 035502. doi:10.1103/PhysRevC.61.035502. nuc1-th/9910008.
- Flambaum VV (1994). Spin hedgehog and collective magnetic quadrupole moments induced by parity and time invariance violating interaction. *Phys. Lett. B* 320: 211–215. doi:10.1016/0370-2693(94)90646-7.
- Flambaum VV, Khriplovich IB and Sushkov OP (1984). On the Possibility to Study  $P$  Odd and  $T$  Odd Nuclear Forces in Atomic and Molecular Experiments. *Sov. Phys. JETP* 60: 873.
- Flambaum VV, Khriplovich IB and Sushkov OP (1986). On the  $P$  and  $T$  Nonconserving Nuclear Moments. *Nucl. Phys. A* 449: 750–760. doi:10.1016/0375-9474(86)90331-3.
- Flambaum VV, DeMille D and Kozlov MG (2014). Time-reversal symmetry violation in molecules induced by nuclear magnetic quadrupole moments. *Phys. Rev. Lett.* 113: 103003. doi:10.1103/PhysRevLett.113.103003. 1406.6479.
- Flambaum VV, Pospelov M, Ritz A and Stadnik YV (2020). Sensitivity of EDM experiments in paramagnetic atoms and molecules to hadronic CP violation. *Phys. Rev. D* 102 (3): 035001. doi:10.1103/PhysRevD.102.035001. 1912.13129.
- Fleig T and Jung M (2018). Model-independent determinations of the electron EDM and the role of diamagnetic atoms. *JHEP* 07: 012. doi:10.1007/JHEP07(2018)012. 1802.02171.
- Froese P and Navrátil P (2021). Ab initio calculations of electric dipole moments of light nuclei. *Phys. Rev. C* 104 (2): 025502. doi:10.1103/PhysRevC.104.025502. 2103.06365.
- Fuyuto K, Ramsey-Musolf M and Shen T (2019). Electric Dipole Moments from CP-Violating Scalar Leptoquark Interactions. *Phys. Lett. B* 788: 52–57. doi:10.1016/j.physletb.2018.11.016. 1804.01137.
- Gandor L, Krebs H and Epelbaum E (2024). Parity and time-reversal violating nuclear forces with explicit  $\Delta$ -excitations. *Eur. Phys. J. A* 60 (10): 211. doi:10.1140/epja/s10050-024-01426-z. 2406.12980.
- Gasser J and Leutwyler H (1984). Chiral Perturbation Theory to One Loop. *Annals Phys.* 158: 142. doi:10.1016/0003-4916(84)90242-2.
- Gaul K and Berger R (2024). Global analysis of  $CP$ -violation in atoms, molecules and role of medium-heavy systems. *JHEP* 08: 100. doi:10.1007/JHEP08(2024)100. 2312.08858.
- Ginges JSM and Flambaum VV (2004). Violations of fundamental symmetries in atoms and tests of unification theories of elementary particles. *Phys. Rept.* 397: 63–154. doi:10.1016/j.physrep.2004.03.005. physics/0309054.
- Gnech A and Viviani M (2020). Time Reversal Violation in Light Nuclei. *Phys. Rev. C* 101 (2): 024004. doi:10.1103/PhysRevC.101.024004. 1906.09021.
- Graner B, Chen Y, Lindahl EG and Heckel BR (2016). Apr. Reduced limit on the permanent electric dipole moment of  $^{199}\text{Hg}$ . *Phys. Rev. Lett.* 116: 161601. doi:10.1103/PhysRevLett.116.161601. <https://link.aps.org/doi/10.1103/PhysRevLett.116.161601>.
- Grzadkowski B, Iskrzynski M, Misiak M and Rosiek J (2010). Dimension-Six Terms in the Standard Model Lagrangian. *JHEP* 10: 085. doi:10.1007/JHEP10(2010)085. 1008.4884.
- Gupta R, Yoon B, Bhattacharya T, Cirigliano V, Jang YC and Lin HW (2018). Flavor diagonal tensor charges of the nucleon from (2+1+1)-flavor lattice QCD. *Phys. Rev. D* 98 (9): 091501. doi:10.1103/PhysRevD.98.091501. 1808.07597.
- Gupta R, Park S, Hoferichter M, Mereghetti E, Yoon B and Bhattacharya T (2021). Pion–Nucleon Sigma Term from Lattice QCD. *Phys. Rev. Lett.* 127 (24): 242002. doi:10.1103/PhysRevLett.127.242002. 2105.12095.
- Haase PAB, Doeglas DJ, Boeschoten A, Eliav E, Iliáš M, Aggarwal P, Bethlem HL, Borschevsky A, Esajas K, Hao Y, Hoekstra S, Marshall VR, Meijknecht TB, Mooij MC, Steinebach K, Timmermans RGE, Touwen AP, Ubachs W, Willmann L and Yin Y (2021). Jul. Systematic study and uncertainty evaluation of  $p$ ,  $t$ -odd molecular enhancement factors in baf. *The Journal of Chemical Physics* 155 (3). ISSN 1089-7690. doi:10.1063/5.0047344. <http://dx.doi.org/10.1063/5.0047344>.
- Haisch U and Hala A (2019). Sum rules for CP-violating operators of Weinberg type. *JHEP* 11: 154. doi:10.1007/JHEP11(2019)154. 1909.08955.
- Hartley AC, Lindroth E and Martensson-Pendrill AM (1990). Parity non-conservation and electric dipole moments in cesium and thallium. *J. Phys. B* 23: 3417–3436.
- Hergert H, Bogner SK, Morris TD, Schwenk A and Tsukiyama K (2016). The In-Medium Similarity Renormalization Group: A Novel Ab Initio Method for Nuclei. *Phys. Rept.* 621: 165–222. doi:10.1016/j.physrep.2015.12.007. 1512.06956.
- Hisano J, Lee JY, Nagata N and Shimizu Y (2012). Reevaluation of Neutron Electric Dipole Moment with QCD Sum Rules. *Phys. Rev. D* 85: 114044. doi:10.1103/PhysRevD.85.114044. 1204.2653.
- Hockings WH and van Kolck U (2005). The Electric dipole form factor of the nucleon. *Phys. Lett. B* 605: 273–278. doi:10.1016/j.physletb.2004.11.043. nuc1-th/0508012.
- Hong DK, Kim HC, Siwach S and Yee HU (2007). The Electric Dipole Moment of the Nucleons in Holographic QCD. *JHEP* 11: 036. doi:10.1088/1126-6708/2007/11/036. 0709.0314.
- Hoogeveen F (1990). The Standard Model Prediction for the Electric Dipole Moment of the Electron. *Nucl. Phys. B* 341: 322–340. doi:10.1016/0550-3213(90)90182-D.
- Hudson JJ, Kara DM, Smallman IJ, Sauer BE, Tarbutt MR and Hinds EA (2011). Improved measurement of the shape of the electron. *Nature* 473: 493–496. doi:10.1038/nature10104.
- Jadbabaie A, Ebadi S, Garcia Ruiz RF, Hutzler NR, Jayich AM and Singh JT (2026), 5. Radioactive Molecules as Laboratories of Fundamental Physics 2605. 12767.
- Jenkins EE and Manohar AV (1991). Baryon chiral perturbation theory using a heavy fermion Lagrangian. *Phys. Lett. B* 255: 558–562. doi:10.1016/0370-2693(91)90266-S.
- Kaplan DB, Savage MJ and Wise MB (1999). A Perturbative calculation of the electromagnetic form-factors of the deuteron. *Phys. Rev. C* 59: 617–629. doi:10.1103/PhysRevC.59.617. nuc1-th/9804032.
- Khriplovich IB and Korokin RA (2000).  $P$  and  $T$  odd electromagnetic moments of deuteron in chiral limit. *Nucl. Phys. A* 665: 365–373. doi:10.1016/S0375-9474(99)00403-0. nuc1-th/9904081.
- Kim J, Luu T, Rizik MD and Shindler A (SymLat) (2021). Nonperturbative renormalization of the quark chromoelectric dipole moment with the gradient flow: Power divergences. *Phys. Rev. D* 104 (7): 074516. doi:10.1103/PhysRevD.104.074516. 2106.07633.
- Kley J, Theil T, Venturini E and Weiler A (2022). Electric dipole moments at one-loop in the dimension-6 SMEFT. *Eur. Phys. J. C* 82 (10): 926. doi:10.1140/epjc/s10052-022-10861-5. 2109.15085.
- Latha KVP, Angom D, Das BP and Mukherjee D (2009). Probing CP violation with the electric dipole moment of atomic mercury. *Phys. Rev. Lett.* 103: 083001. doi:10.1103/PhysRevLett.103.083001. [Erratum: *Phys.Rev.Lett.* 115, 059902 (2015)], 0902.4790.
- Liang J, Alexandru A, Draper T, Liu KF, Wang B, Wang G and Yang YB ( $\chi$ QCD) (2023). Nucleon electric dipole moment from the  $\theta$  term with lattice chiral fermions. *Phys. Rev. D* 108 (9): 094512. doi:10.1103/PhysRevD.108.094512. 2301.04331.
- Liu KF (2025). Lattice QCD and the Neutron Electric Dipole Moment. *Ann. Rev. Nucl. Part. Sci.* 75 (1): 377–397. doi:10.1146/annurev-nucl-121423-100927. 2411.15198.

- Liu CP and Timmermans RGE (2004). P- and T-odd two-nucleon interaction and the deuteron electric dipole moment. *Phys. Rev. C* 70: 055501. doi:10.1103/PhysRevC.70.055501. nucl-th/0408060.
- Liu CP, de Vries J, Mereghetti E, Timmermans RGE and van Kolck U (2012). Deuteron Magnetic Quadrupole Moment From Chiral Effective Field Theory. *Phys. Lett. B* 713: 447–452. doi:10.1016/j.physletb.2012.06.024. 1203.1157.
- Lüscher M (2010). Properties and uses of the Wilson flow in lattice QCD. *JHEP* 08: 071. doi:10.1007/JHEP08(2010)071. [Erratum: *JHEP* 03, 092 (2014)], 1006.4518.
- Maekawa CM, Mereghetti E, de Vries J and van Kolck U (2011). The Time-Reversal- and Parity-Violating Nuclear Potential in Chiral Effective Theory. *Nucl. Phys. A* 872: 117–160. doi:10.1016/j.nuclphysa.2011.09.020. 1106.6119.
- Manohar A and Georgi H (1984). Chiral Quarks and the Nonrelativistic Quark Model. *Nucl. Phys. B* 234: 189–212. doi:10.1016/0550-3213(84)90231-1.
- Mereghetti E, Hockings WH and van Kolck U (2010). The Effective Chiral Lagrangian From the Theta Term. *Annals Phys.* 325: 2363–2409. doi:10.1016/j.aop.2010.03.005. 1002.2391.
- Mereghetti E, de Vries J, Hockings WH, Maekawa CM and van Kolck U (2011). The Electric Dipole Form Factor of the Nucleon in Chiral Perturbation Theory to Sub-leading Order. *Phys. Lett. B* 696: 97–102. doi:10.1016/j.physletb.2010.12.018. 1010.4078.
- Mereghetti E, Monahan CJ, Rizik MD, Shindler A and Stoffer P (2022). One-loop matching for quark dipole operators in a gradient-flow scheme. *JHEP* 04: 050. doi:10.1007/JHEP04(2022)050. [Erratum: *JHEP* 03, 101 (2025)], 2111.11449.
- Mulder H, Timmermans R and de Vries J (2025). Probing the QCD  $\bar{\theta}$  term with paramagnetic molecules. *JHEP* 07: 232. doi:10.1007/JHEP07(2025)232. 2502.06406.
- Naterop L and Stoffer P (2026). Renormalization-group equations of the LEFT at two loops: dimension-six operators. *JHEP* 02: 016. doi:10.1007/JHEP02(2026)016. 2507.08926.
- Nelson AE (1984). Naturally Weak CP Violation. *Phys. Lett. B* 136: 387–391. doi:10.1016/0370-2693(84)92025-2.
- Ng J and Tulin S (2012). D versus d: CP Violation in Beta Decay and Electric Dipole Moments. *Phys. Rev. D* 85: 033001. doi:10.1103/PhysRevD.85.033001. 1111.0649.
- Ng KB, Foster S, Cheng L, Navratil P and Malbrunot-Ennenauer S (2026). Nuclear Schiff Moment of the Fluorine Isotope F19. *Phys. Rev. Lett.* 136 (11): 112501. doi:10.1103/m4fx-g1h6. 2507.19811.
- Nogga A, Timmermans RGE and van Kolck U (2005). Renormalization of one-pion exchange and power counting. *Phys. Rev. C* 72: 054006. doi:10.1103/PhysRevC.72.054006. nucl-th/0506005.
- Nogga A, Fonseca AC, Gardestig A, Hanhart C, Horowitz CJ, Miller GA, Niskanen JA and van Kolck U (2006). Realistic few-body physics in the  $dd \rightarrow \alpha \pi$  reaction. *Phys. Lett. B* 639: 465–470. doi:10.1016/j.physletb.2006.04.058. nucl-th/0602003.
- Ottnad K, Kubis B, Meissner UG and Guo FK (2010). New insights into the neutron electric dipole moment. *Phys. Lett. B* 687: 42–47. doi:10.1016/j.physletb.2010.03.005. 0911.3981.
- Peccei RD and Quinn HR (1977). CP Conservation in the Presence of Instantons. *Phys. Rev. Lett.* 38: 1440–1443. doi:10.1103/PhysRevLett.38.1440.
- Porsev SG, Safronova MS and Kozlov MG (2012). Electric dipole moment enhancement factor of thallium. *Phys. Rev. Lett.* 108: 173001. doi:10.1103/PhysRevLett.108.173001. 1201.5615.
- Pospelov M (2002). Best values for the CP odd meson nucleon couplings from supersymmetry. *Phys. Lett. B* 530: 123–128. doi:10.1016/S0370-2693(02)01263-7. hep-ph/0109044.
- Pospelov M and Ritz A (1999). Theta induced electric dipole moment of the neutron via QCD sum rules. *Phys. Rev. Lett.* 83: 2526–2529. doi:10.1103/PhysRevLett.83.2526. hep-ph/9904483.
- Pospelov M and Ritz A (2001). Neutron EDM from electric and chromoelectric dipole moments of quarks. *Phys. Rev. D* 63: 073015. doi:10.1103/PhysRevD.63.073015. hep-ph/0010037.
- Pospelov M and Ritz A (2014). CKM benchmarks for electron electric dipole moment experiments. *Phys. Rev. D* 89 (5): 056006. doi:10.1103/PhysRevD.89.056006. 1311.5537.
- Pospelov M and Ritz A (2025). 9. Electric Dipole Moments and New Physics 2509.23531.
- Roussy TS and et al. (2023). An improved bound on the electron's electric dipole moment. *Science* 381 (6653): adg4084. doi:10.1126/science.adg4084. 2212.11841.
- Sandars PGH (1965). The electric dipole moment of an atom. *Phys. Lett.* 14 (3): 194–196. doi:10.1016/0031-9163(65)90583-4.
- Sandars P (1966). Enhancement factor for the electric dipole moment of the valence electron in an alkali atom. *Physics Letters* 22 (3): 290–291. ISSN 0031-9163. doi:https://doi.org/10.1016/0031-9163(66)90618-4. <https://www.sciencedirect.com/science/article/pii/0031916366906184>.
- Schiff LI (1963). Measurability of Nuclear Electric Dipole Moments. *Phys. Rev.* 132: 2194–2200. doi:10.1103/PhysRev.132.2194.
- Seng CY, de Vries J, Mereghetti E, Patel HH and Ramsey-Musolf M (2014). Nucleon electric dipole moments and the isovector parity- and time-reversal-odd pion–nucleon coupling. *Phys. Lett. B* 736: 147–153. doi:10.1016/j.physletb.2014.07.014. 1401.5366.
- Shindler A (2021). Flavor-diagonal CP violation: the electric dipole moment. *Eur. Phys. J. A* 57 (4): 128. doi:10.1140/epja/s10050-021-00421-y.
- Skripnikov LV (2017). Communication: Theoretical study of HfF<sup>+</sup> cation to search for the T,P-odd interactions. *J. Chem. Phys.* 147 (2): 021101. doi:10.1063/1.4993622.
- Song YH, Lazauskas R and Gudkov V (2013). Nuclear electric dipole moment of three-body systems. *Phys. Rev. C* 87 (1): 015501. doi:10.1103/PhysRevC.87.015501. 1211.3762.
- Spevak V and Auerbach N (1995). Parity mixing and time reversal violation in nuclei with octupole deformations. *Phys. Lett. B* 359: 254–260. doi:10.1016/0370-2693(95)01099-C.
- Stetcu I, Liu CP, Friar JL, Hayes AC and Navratil P (2008). Nuclear Electric Dipole Moment of He-3. *Phys. Lett. B* 665: 168–172. doi:10.1016/j.physletb.2008.06.019. 0804.3815.
- Sushkov OP and Flambaum VV (1978). Parity Violation Effects in Diatomic Molecules. *Sov. Phys. JETP* 48: 608.
- 't Hooft G (1976). Symmetry Breaking Through Bell-Jackiw Anomalies. *Phys. Rev. Lett.* 37: 8–11. doi:10.1103/PhysRevLett.37.8.
- Thomas SD (1995). Electromagnetic contributions to the Schiff moment. *Phys. Rev. D* 51: 3955–3957. doi:10.1103/PhysRevD.51.3955. hep-ph/9402237.
- van de Vis J, de Vries J and Postma M (2026). Bubble Trouble: a Review on Electroweak Baryogenesis. *Prog. Part. Nucl. Phys.* 150: 104244. doi:10.1016/j.pnpnp.2026.104244. 2508.09989.
- van Kolck U (2020a). Naturalness in nuclear effective field theories. *Eur. Phys. J. A* 56 (3): 97. doi:10.1140/epja/s10050-020-00092-1. 2003.09974.
- van Kolck U (2020b). The Problem of Renormalization of Chiral Nuclear Forces. *Front. in Phys.* 8: 79. doi:10.3389/fphy.2020.00079. 2003.06721.
- van Kolck U, Niskanen JA and Miller GA (2000). Charge symmetry violation in  $p n \rightarrow d \pi$  as a test of chiral effective field theory. *Phys. Lett. B* 493: 65–72. doi:10.1016/S0370-2693(00)01133-3. nucl-th/0006042.
- Weinberg S (1979). Phenomenological Lagrangians. *Physica A* 96 (1-2): 327–340. doi:10.1016/0378-4371(79)90223-1.

- Weinberg S (1989). Larger Higgs Exchange Terms in the Neutron Electric Dipole Moment. *Phys. Rev. Lett.* 63: 2333. doi:10.1103/PhysRevLett.63.2333.
- Weinberg S (1990). Nuclear forces from chiral Lagrangians. *Phys. Lett. B* 251: 288–292. doi:10.1016/0370-2693(90)90938-3.
- Xu F, An H and Ji X (2010). Neutron Electric Dipole Moment Constraint on Scale of Minimal Left-Right Symmetric Model. *JHEP* 03: 088. doi:10.1007/JHEP03(2010)088. 0910.2265.
- Yamada T, Funaki Y, Horiuchi H, Roepke G, Schuck P and Tohsaki A (2012). Nuclear Alpha-Particle Condensates. *Lect. Notes Phys.* 848: 229–298. doi:10.1007/978-3-642-24707-1\_5. 1103.3940.
- Yamaguchi Y and Yamanaka N (2020). Large long-distance contributions to the electric dipole moments of charged leptons in the standard model. *Phys. Rev. Lett.* 125: 241802. doi:10.1103/PhysRevLett.125.241802. 2003.08195.
- Yamanaka N (2017). Review of the electric dipole moment of light nuclei. *Int. J. Mod. Phys. E* 26 (4): 1730002. doi:10.1142/S0218301317300028. 1609.04759.
- Yamanaka N and Hiyama E (2015). Enhancement of the CP-odd effect in the nuclear electric dipole moment of  ${}^6\text{Li}$ . *Phys. Rev. C* 91 (5): 054005. doi:10.1103/PhysRevC.91.054005. 1503.04446.
- Yamanaka N and Hiyama E (2021). Weinberg operator contribution to the nucleon electric dipole moment in the quark model. *Phys. Rev. D* 103 (3): 035023. doi:10.1103/PhysRevD.103.035023. 2011.02531.
- Yamanaka N, Yamada T and Funaki Y (2019). Nuclear electric dipole moment in the cluster model with a triton:  ${}^7\text{Li}$  and  ${}^{11}\text{B}$ . *Phys. Rev. C* 100 (5): 055501. doi:10.1103/PhysRevC.100.055501. 1907.08091.
- Yanase K and Shimizu N (2020). Large-scale shell-model calculations of nuclear Schiff moments of  ${}^{129}\text{Xe}$  and  ${}^{199}\text{Hg}$ . *Phys. Rev. C* 102 (6): 065502. doi:10.1103/PhysRevC.102.065502. 2006.15142.
- Yang Z, Mereghetti E, Platter L, Schindler MR and Vanasse J (2021). Electric dipole moments of three-nucleon systems in the pionless effective field theory. *Phys. Rev. C* 104 (2): 024002. doi:10.1103/PhysRevC.104.024002. 2011.01885.
- Zhou EF, Yao JM, Engel J and Meng J (2025), 7. Effects of beyond-mean-field correlations on nuclear Schiff moments 2507.01369.